PHYSICAL ASPECTS OF 5-D GRAVITY

By

Andrew Philip Billyard

A thesis

presented to the University of Waterloo

in fulfilment of the

thesis requirement for the degree of

Master of Science

in

Physics

Waterloo, Ontario, Canada, 1995

© Andrew Philip Billyard, 1995

I hereby declare that I am the sole author of this thesis.

I authorize the University of Waterloo to lend this thesis to other institutions or individuals for the purpose of scholarly research.

I further authorize the University of Waterloo to reproduce this thesis by photocopying or by other means, in total of in part, at the request of other institutions of individuals for the purpose of scholarly research.

The University of Waterloo requires the signatures of all persons using or photocopying this thesis. Please sign below, and give address and date.

Physical Aspects of 5-D Gravity

Abstract

In Kaluza-Klein theory, spacetime is extended to dimensions greater than four; the simplest version is one in which the augmentation is just by one extra dimension. The existence of this dimension can be tested over different astronomical scales, and we outline various physical aspects found on these scales. On the stellar scale, we look at a (4+1) class of solutions analogous to the (3+1) Schwarzschild solution. In general, the (4+1) centre is actually located at the (3+1) event horizon. The radii of circular orbits in these manifolds have a much greater range than in the (3+1) solution and in some cases the entire manifold. Furthermore, in some cases we see that photons can have stable circular orbits. Next, we derive a solution that is spherically-symmetric in ordinary 3-D space, but is also dependent on the extra coordinate. In the induced-matter theory, where the extra dimension is responsible for matter in the 4-D spacetime, the solution represents a cloud of matter with density and pressure profiles similar to that of a rich cluster of galaxies. The motion of particles inside the manifold is then derived. On the largest scale, we derive a cosmological solution with an oscillating 3-D spatial section which, in the induced-matter scheme, has a vacuum equation of state. From this solution we can also get an inflationary cosmology. We also show that coordinate transformations from a 5-D "Minkowski" spacetime can produce various cosmological models.

Acknowledgments

I am indebted to my supervisor, Paul Wesson, for his continuous guidance and support throughout this work. I would also like to thank Jamie Ponce de Leon, Robb Mann, Dimitri Kalligas, Bill Sajko and Catalina Alvarez for enlightening discussions.

Much support and kind service was received from the staff of the Physics Graduate Department and so I thank Teresa Glaves, Sabine Kawalec and Debbie Guenter. My appreciation extends also to Eric Howe for his assistance with many computer details and to Kayll Lake for his software GRTensor.

This research was funded by the National Science and Engineering Research Council of Canada (NSERC) with an NSERC PGS-A scholarship.

Table of Contents

Abstract **iv**

Acknowledgments **v**

List of Figures **viii**

1 Introduction **1**

2 The Solitons **7**

2.1 Definition of Origin 7

2.2 Geodesic Motion 12

2.3 Stability of Circular Orbits 19

2.3.1 Massless particles ($\Xi = 0$) with $V_0 = 0$ for all (ϵ, κ) . . . 22

2.3.2 Schwarzschild limit $(\epsilon, \kappa) = (0, \infty)$ 23

2.3.3 Chatterjee case $(\epsilon, \kappa) = (1, 1)$ 24

2.3.4 "Synchronous" case $(\epsilon, \kappa) = (1, 0)$ 25

2.3.5 Circular Orbits for $1 < \kappa < \infty$ 27

2.3.6 Circular Orbits for $0 < \kappa < 1$ 30

3 Isotrope Solutions **32**

3.1 Static, Inhomogeneous Isothermal Solutions 32

3.2 Geodesic Motion 38

4 Vacuum Waves **45**

4.1 Cosmological Models from Flat Space-times 45

4.2 Geodesic Motion 50

5 Conclusions **54**

A Christoffel Symbols and Riemann Tensor Components **58**

B Subroutines Written for MapleV **62**

References **69**

List of Figures

2.1 Transformation between radial and isotropic co-ordinates 10

2.2 Energy of particle, $\dot{t}$, as a function of isotropic r 15

2.3 Radial velocity of particle as a function of isotropic r 16

2.4 "Psi" velocity, $\dot{\psi}$, as a function of isotropic r 17

2.5 Proper size of fifth dimension for a radially travelling particle, ψ_{prop}, as a function of proper distance, R_{prop} 19

2.6 General form of F_2, or $\tilde{f}'(\tilde{r})$ with $\Xi = 0$ and $V_0 = 0$. 28

3.1 Ratio of pressure to density, p/ρ, for 4-D and 5-D models. . . . 36

Chapter 1

Introduction

The idea of extending general relativity to greater dimensions has been around for many years, almost as early as the theory of relativity itself. In 1921, Kaluza [1] extended general relativity to five dimensions in an attempt to unite gravity with electromagnetism, where the extended off-diagonal components of the metric were related to the electromagnetic vector field and the diagonal metric component of the fifth dimension was a scalar potential. In 1926, this idea was further developed by Klein [2] to apply it to quantum mechanics. Often, any theory which extends general relativity to dimensions greater than four is referred to as Kaluza-Klein theory.

Klein originally introduced the notion of compactification in order to explain why the extra dimension is not observable; the extra dimension is "rolled"

up such that it is unobservable unless small distances or high energies are considered. Albeit quaint, this theory led to several problems. First there is the hierarchy problem where the natural mass of particles associated with the fifth dimension is the Planck mass which is far larger than the masses of real particles. Secondly, the cosmological constant calculated from the reduction of higher dimensions to four is far larger than that indicated by astrophysical data.

These problems may be avoided in non-compact Kaluza-Klein theory, on which there is considerable literature. Perhaps the most studied such version is the induced matter one, in which the vacuum solutions in five dimensions (5-D) are interpreted as solutions with matter in four dimensions (4-D), providing a unification of gravity with its source. This theory plays a significant role in this paper. The vacuum in five dimensions is described by $R_{AB} = 0$, where R_{AB} is the Ricci tensor in 5-D. These fifteen equations contain ten equations of the form ${}^{(4)}G_{\alpha\beta} = {}^{(4)}T_{\alpha\beta}$, where the left side is the (3+1) Einstein tensor and the right side is the (3+1) effective energy-momentum tensor which comprises terms due to the extra dimension (i.e. 5-D portion of the metric and derivatives with respect to the extra dimension). The remaining five equations comprise one wave equation and four conservation equations. The notation here and throughout, unless otherwise stated, is that units are such that $c = 8\pi G = 1$.

Furthermore, uppercase Latin indices range 0-4, lowercase Greek range 0-3 and lowercase Latin range 1-3.

In this particular theory, the extra metric components are not usually associated with an electromagnetic potential. In fact, the off-diagonal components of the metric $g_{\alpha 4}$ are zero. Further distinctions from the traditional Kaluza-Klein approach is that the signature of the fifth dimension can be positive or negative because the extra coordinate is not a simple space or time label, but a variable related to the properties of 4-D matter in a 5-D vacuum and so there is a freedom to the choice of signature. In previous work [3]-[8] the extra coordinate is associated with the rest mass of particles and the signature then determines whether the mass increases or decreases over time [6]. In this thesis, some solutions require a spacelike signature in order to have a 5-D vacuum (and in some cases a completely flat metric), and others a timelike signature. Dependence on the extra coordinate is also a difference from conventional Kaluza-Klein. This is particularly interesting since it has been shown that metrics dependent solely on the radial coordinate give an induced equation of state for radiation only [9].

This paper will examine three different metrics, each with a different astronomical scale involved: solar size, galactic cluster size and cosmological. On the first scale, we examine the (4+1) analogue to the (3+1) Schwarzschild solution.

Unlike the (3+1) theory, Birkhoff's theorem does not hold with 3-D spherical symmetry here. Consequently, there is not a unique solution, but a class of solutions parameterized by two constants, ϵ and κ, which obey a consistency relationship between one another. The Schwarzschild limit is smoothly retrieved with $\kappa \rightarrow \infty, \epsilon = 0, \epsilon\kappa = 1$. This limit returns the (3+1) Schwarzschild metric plus a flat fifth dimension. Should $\epsilon \neq 0$, then the fifth dimension becomes significant and the event horizon disappears [10]-[14]. Because of the lack of horizon, it would be inappropriate to label these objects as black holes. Instead, they represent a stable mass centrally located, and better fit the definition of a soliton from particle physics [15] for which they are here called solitons. It is possible to test the significance of an extra dimension outside such objects as the Sun and the Earth, and such tests are currently being explored [17, 16]. Much work has already been done on these solutions, including a study on classical tests in these manifolds [17] and an in-depth induced-matter analysis [20]. Because of the latter, this paper will not focus on that particular aspect of the theory. Instead, we examine where the origin of these solitons are defined. This is then followed by an examination of the effects of ϵ and κ as well as momentum in the fifth dimension on circular orbits.

In chapter 3, we next determine another class of solutions that are also

spherically symmetrical, but which also depend on the extra coordinate. In the induced matter scheme, we find a density and pressure relationship similar to those of rich clusters of galaxies; i.e. static, inhomogeneous isothermal solutions with density and pressure proportional to r^{-2}. This metric, describing objects called isotropes, is the 5-D analogue to the 4-D astrophysical solution studied by Henriksen and Wesson [23, 24]. We then examine the motion of particles in this manifold which we hope to use later for gravitational lens calculations.

In chapter 4, we find a metric which contains a vacuum equation of state. Although the vacuum is unperturbed, the spatial portion of the metric is oscillating and so the metric describes what have been called vacuum waves. Upon making the angular frequency complex, the metric looks like an inflationary cosmology on hypersurfaces of $x^4 = \psi = constant$. We also show that this metric can be transformed into a flat "Minkowski" metric, and the same can be done for other cosmological models previously studied. The conclusions are summarized in chapter 5.

Appendix A contains the Christoffel symbols (of the second kind) for all the metrics used in this thesis. It also gives the Riemann tensor components for the solitons. Many calculations were performed or checked by the software package Maple V, supplemented with the library GRTensor by Kayll Lake. Appendix

B contains a few subroutines that were written and used with the Maple V software. The file mentioned in appendix B can be found on a 3.5″ floppy at the back of the thesis.

Chapter 2

The Solitons

2.1 Definition of Origin

Using the notation adopted by Davidson and Owen [11], the line interval describing the spherically-symmetric, static, five-dimensional vacuum surrounding a central massive object is given by

$$ds^2 = A^2(r)dt^2 - B^2(r)(dr^2 + r^2 d\Omega^2) - C^2(r)d\psi^2, \tag{2.1}$$

where

$$A(r) = \left(\frac{ar-1}{ar+1}\right)^{\epsilon\kappa} \tag{2.2}$$

$$B(r) = \left(\frac{a^2r^2-1}{a^2r^2}\right)\left(\frac{ar+1}{ar-1}\right)^{\epsilon(\kappa-1)} \tag{2.3}$$

$$C(r) = \left(\frac{ar+1}{ar-1}\right)^{\epsilon}. \tag{2.4}$$

Here, $d\Omega^2 \equiv d\theta^2 + \sin^2\theta d\phi^2$ and the units are geometric so that $c = G = 1$. The integration constant, a, is associated geometrically with the central object and is often expressed as $a = \frac{2}{M}$, where M is a mass, to more closely resemble the 4-D Schwarzschild analogue. The other two constants, ϵ and κ, obey the relation $\epsilon^2(\kappa^2 - \kappa + 1) = 1$ as established from the field equations, $R_{AB} = 0$. For the range $-\infty < \kappa < \infty$, ϵ ranges between $\pm\frac{2}{\sqrt{3}}$. However, ϵ and κ must have positive values so that the associated 4-D pressure and density, as well as mass, are positive [19]. Since these solitons described by (2.1) provide a good astrophysical model, we will assume that both ϵ and κ remain positive.

As the line interval (2.1) is in isotropic co-ordinates, it is sometimes convenient to transform it into one which uses quasi-curvature co-ordinates, by which the 4-D Schwarzschild metric is most commonly described. The transformation is given by

$$\tilde{r} = rB(r) = r\frac{a^2r^2 - 1}{a^2r^2}\left(\frac{ar+1}{ar-1}\right)^{\epsilon(\kappa-1)}. \tag{2.5}$$

Since $\epsilon(\kappa-1)$ is not necessarily an integer, it is not possible to obtain $r(\tilde{r})$ explicitly so that (2.1) cannot be expressed in terms of $\tilde{r}$ for all (ϵ, κ). However, as the limits $(\epsilon, \kappa, \epsilon\kappa) \to (0, \infty, 1)$ are approached, (2.1) becomes the 4-D Schwarzschild solution plus a flat fifth dimension. Using (2.5) in this limit, $\tilde{r} = r(1 + \frac{1}{ar})^2$, we

have (with $a = \frac{2}{M}$)

$$ds^2 = \left(1 - \frac{2M}{\tilde{r}}\right) dt^2 - \left(1 - \frac{2M}{\tilde{r}}\right)^{-1} d\tilde{r}^2 - \tilde{r}^2 d\Omega^2 - d\psi^2. \tag{2.6}$$

Here, we have an event horizon at $\tilde{r} = 2M = \frac{4}{a}$ (or $r = \frac{1}{a} = \frac{M}{2}$) and a singularity at $\tilde{r} = 0$ ($r = -\frac{1}{a}$).

A suitable definition of an origin is a point in the manifold about which the surface area of a 3-sphere will shrink to zero. From the consistency relation $\epsilon^2(\kappa^2 - \kappa + 1) = 1$, it may be verified that $-1 \leq \epsilon(\kappa - 1) < 1$ for all finite $\kappa \geq 0$ and therefore the 3-D angular portion of (2.1) converges to a point at both $r = \pm\frac{1}{a}$. It is then natural to ask which value of r does one choose as the origin. In previous work [20] $r = \frac{1}{a}$ was taken as the origin, even though (2.6) admits $r = -\frac{1}{a}$ as the origin.

Figure 2.1 shows a graphical representation of (2.5) for various values of $\epsilon(\kappa - 1)$. For all values of $\epsilon(\kappa - 1) < 1$ it is apparent that $r = \frac{1}{a}$ corresponds to the "quasi-curvature co-ordinate" centre, $\tilde{r} = 0$. Only for $\epsilon(\kappa - 1) = 1$ is this not so. However, in this Schwarzschild limit, $(\epsilon, \kappa, \epsilon\kappa) \to (0, \infty, 1)$, there is no region of r which covers the region interior to the 4-D event horizon, $\tilde{r} = 2M$. In fact, $0 \leq r \leq \frac{1}{a}$ merely represents $\tilde{r} \geq 2M$ again and $\tilde{r} = 0$ can be obtained only through $r < 0$. Hence, on these physical grounds, $r = \frac{1}{a}$ will be taken as the

origin of (2.1) for all $\kappa \geq 0$.

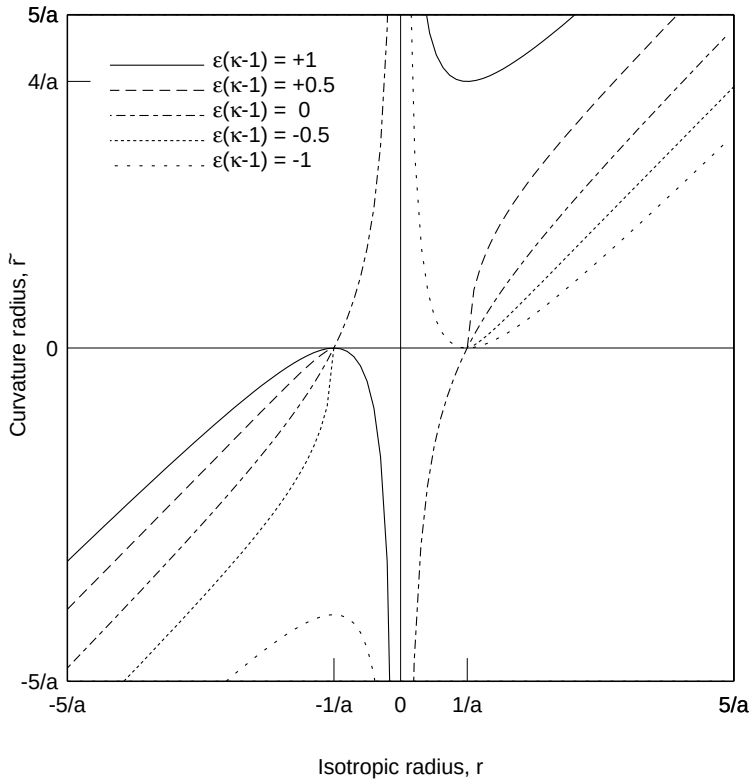

Figure 2.1: Transformation between radial and isotropic co-ordinates

We calculated the Kretschmann full curvature invariant scalar for (2.1) by hand and then affirmed the result via the software packages GRTensor and Maple V. From (2.1) we have

$$\begin{aligned} R_{ABCD}R^{ABCD} &= 4\frac{(A'')^2}{A^2B^4} - 8\frac{A''A'B'}{A^2B^5} + 12\frac{(A')^2(B')^2}{A^2B^6} + 16\frac{(A')^2B'}{rA^2B^5} \\ &\quad +8\frac{(A')^2}{r^2A^2B^4} + 4\frac{(A')^2(C')^2}{A^2B^4C^2} + 12\frac{(B')^4}{B^8} - 16\frac{(B')^2B''}{B^7} \\ &\quad +24\frac{(B')^2}{r^2B^6} + 16\frac{B'B''}{rB^6} + 8\frac{(B'')^2}{B^6} + 4\frac{(C'')^2}{B^4C^2} \end{aligned}$$

$$-8\frac{B'C'C''}{B^5C^2}+12\frac{(B')^2(C')^2}{B^6C^2}+16\frac{B'(C')^2}{rB^5C^2}+8\frac{(C')^2}{r^2B^4C^2}$$

where $A' \equiv \partial A(r)/\partial r$ etc. (the Christoffel symbols and the Riemann tensor components for (2.1) can be found in Appendix A). Substituting in for A, B and C, the scalar simplifies to

$$\begin{aligned} R_{ABCD}R^{ABCD} &= \frac{192a^{10}r^6}{(a^2r^2-1)^8}\left(\frac{ar-1}{ar+1}\right)^{4\epsilon(\kappa-1)} \times \\ &\quad [1-2\epsilon(\kappa-1)(2+\epsilon^2\kappa)ar+2(3-\epsilon^4\kappa^2)a^2r^2 \\ &\quad -2\epsilon(\kappa-1)(2+\epsilon^2\kappa)a^3r^3+a^4r^4] \end{aligned} \tag{2.7}$$

For all finite κ there is a divergence at both $r=\pm\frac{1}{a}$. Again, if we take $r=\frac{1}{a}$ as the origin, then one must go through the singularity at $r=\frac{1}{a}$ to the second singularity at $r=-\frac{1}{a}$ and hence the latter can be regarded as unphysical. In the Schwarzschild limit, (2.7) becomes $R_{ABCD}R^{ABCD}=48M^2/\tilde{r}^6$ (using (2.5)) which is the standard 4-D general relativistic value. The singularity at $r=\frac{1}{a}$ seems to disappear in this limit, but otherwise exists providing there is even the slightest curvature in the fifth dimension, ($\epsilon \neq 0$). Thus, (2.7) clearly indicates a geometrical singularity at $r=\frac{1}{a}$, provided the fifth dimension is significant.

Conversely, the 4-D Schwarzschild limit, $(\epsilon,\kappa,\epsilon\kappa)\rightarrow(0,\infty,1)$, has a geometrical singularity at $r=-\frac{1}{a}$ ($\tilde{r}=0$). However, this is no longer part of the manifold in the 5-D picture, which ends at $r=\frac{1}{a}$ or $\tilde{r}=2M$. In other words, the

horizon of the 4-D solution becomes the centre of the 5-D solution.

2.2 Geodesic Motion

Consider the five geodesic equations,

$$\frac{d^2x^A}{ds^2} + \Gamma^A_{BC}\frac{dx^B}{ds}\frac{dx^C}{ds} = 0$$

for the interval (2.1):

$$\frac{d\dot{t}}{ds} + 2\frac{A'}{A}\dot{t}\dot{r} = 0 \tag{2.8}$$

$$\frac{d\dot{r}}{ds} + \frac{AA'}{B^2}\dot{t}^2 + \frac{B'}{B}\dot{r}^2 - \left(r^2\frac{B'}{B} + r\right)\left[\dot{\theta}^2 + \sin^2\theta\,\dot{\phi}^2\right] - \frac{CC'}{B^2}\dot{\psi}^2 = 0 \tag{2.9}$$

$$\frac{d\dot{\theta}}{ds} + 2\left(\frac{B'}{B} + \frac{1}{r}\right)\dot{r}\dot{\theta} - \sin\theta\cos\theta\dot{\phi}^2 = 0 \tag{2.10}$$

$$\frac{d\dot{\phi}}{ds} + 2\left(\frac{B'}{B} + \frac{1}{r}\right)\dot{r}\dot{\phi} + 2\frac{\cos\theta}{\sin\theta}\dot{\theta}\dot{\phi} = 0 \tag{2.11}$$

$$\frac{d\dot{\psi}}{ds} + 2\frac{C'}{C}\dot{\psi}\dot{r} = 0 \tag{2.12}$$

where $\dot{t} \equiv \frac{dx^0}{ds}$, $\dot{r} \equiv \frac{dx^1}{ds}$, $\dot{\theta} \equiv \frac{dx^2}{ds}$, $\dot{\phi} \equiv \frac{dx^3}{ds}$, $\dot{\psi} \equiv \frac{dx^4}{ds}$, and A, B and C are defined in (2.2)-(2.4).

Equations (2.8) and (2.12) are almost trivial to solve. In fact, $\dot{t}$, $\dot{\phi}$ and $\dot{\psi}$ can be solved by noting that $\partial/\partial t$, $\partial/\partial\phi$ and $\partial/\partial\psi$ are all Killing vectors, ξ^A, and therefore constants of motion (w.r.t. s) can be obtained from $k(constant) =$

$g_{AB}\xi^A \frac{dx^B}{ds}$. Equations (2.10) and (2.11) can be made identical by assuming $\theta = f(\theta)\phi$ and then solving for $f(\theta)$ obtains $\dot{\theta}$. Finally, $\dot{r}$ can be found by the consistency relation $\Xi = g_{AB}\frac{dx^A}{ds}\frac{dx^B}{dx}$ which is obtained by dividing (2.1) by ds^2. The constant Ξ is 1 or 0 for massive or massless particles (respectively). The resulting velocities are hence:

$$\dot{t} = \frac{E}{A^2} \tag{2.13}$$

$$\dot{r} = \frac{\pm 1}{B}\sqrt{\frac{E^2}{A^2} - \frac{WL^2}{B^2r^2} - \frac{V_0^2}{C^2} - \Xi} \tag{2.14}$$

$$\begin{aligned} \dot{\theta} &= \sin^2\theta\sqrt{W - \csc^2\theta}\ \dot{\phi} \\ &= \frac{L}{B^2r^2}\sqrt{W - \csc^2\theta} \end{aligned} \tag{2.15}$$

$$\dot{\phi} = \frac{L}{B^2r^2}\csc^2\theta \tag{2.16}$$

$$\dot{\psi} = \frac{V_0}{C^2} \tag{2.17}$$

and can be verified by substituting back into (2.8)-(2.12). The constants E, L, and V_0 are integration constants and constants of motion. The constant W in (2.14) and (2.15) is another integration constant. Typically, since these solutions are spherically symmetric and the motion will lie in one plane, it is practice to first set $\theta = \pi/2$ and $\dot{\theta} = 0$ before solving the geodesics ((2.10) will automatically be satisfied), and so $W = 1$ in this case.

It is easily seen that $\dot{t}$, $\dot{\phi}$ and $\dot{\theta}$ are identical to the standard 4-D general

relativistic velocities in the Schwarzschild limit. However, $\dot{r}$ and $\dot{\psi}$ will still retain a constant V_0; in this limit, $\dot{r}^2$ is lower than the 4-D general relativistic value by a factor $V_0^2\left(1+\frac{1}{ar}\right)^2$.

There is a bound to $\dot{r}$ evident from (2.14),

$$E^2 \geq WL^2\frac{A^2}{B^2r^2} + V_0^2\frac{A^2}{C^2} - A^2\Xi,$$

which is to say that a particle cannot be at radius r from the soliton unless this condition is satisfied. Hence, in order for a particle to escape to infinity, $E^2 \geq V_0^2 + \Xi$, which is more energy needed than in the 4-D case where the condition would be $E^2 \geq \Xi$.

Figures 2.2, **2.3** and **2.4** depict the energy, $\dot{t}$, the radial velocity, $\dot{r}$, and the "psi" velocity, $\dot{\psi}$, (respectively) of a massive particle ($\Xi = 1$) falling radially ($L = 0$) into the soliton (with $V_0 = .25$ and $E = 1.25$). As in the 4-D Schwarzschild solution, the energy of the particle diverges at it approaches $r = \frac{1}{a}$, as well as the radial velocity. The difference, however, is that the divergence occurs at the event horizon in 4-D and at the origin in 5-D.

The velocities $\dot{\theta}$ and $\dot{\phi}$ are not plotted for they can be made to look identical to their 4-D Schwarzschild counterparts, providing the transformation (2.5) is made. Although this would appear to contradict earlier work distinguishing the

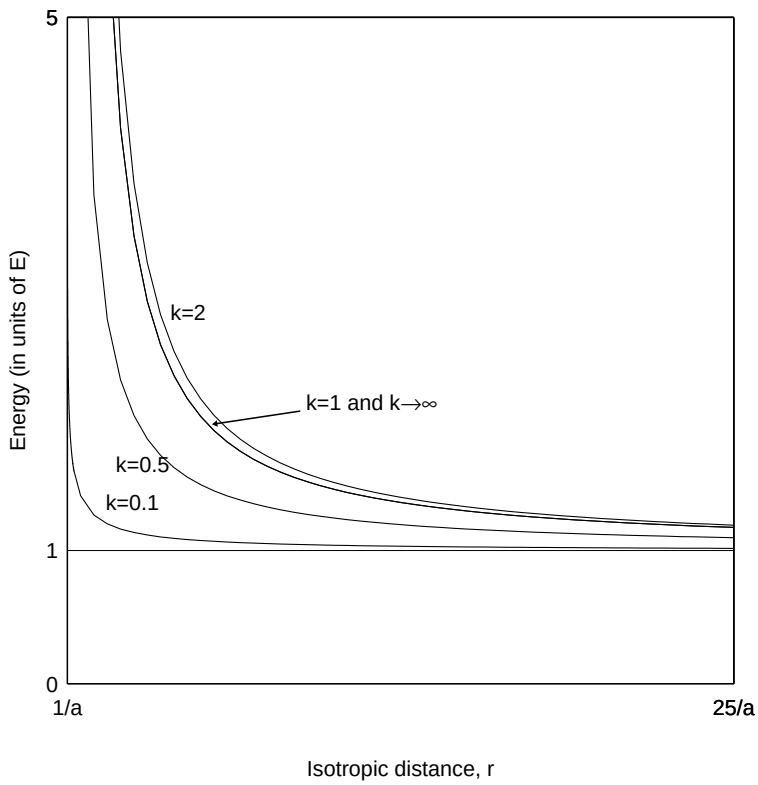

Figure 2.2: Energy of particle, $\dot{t}$, as a function of isotropic r

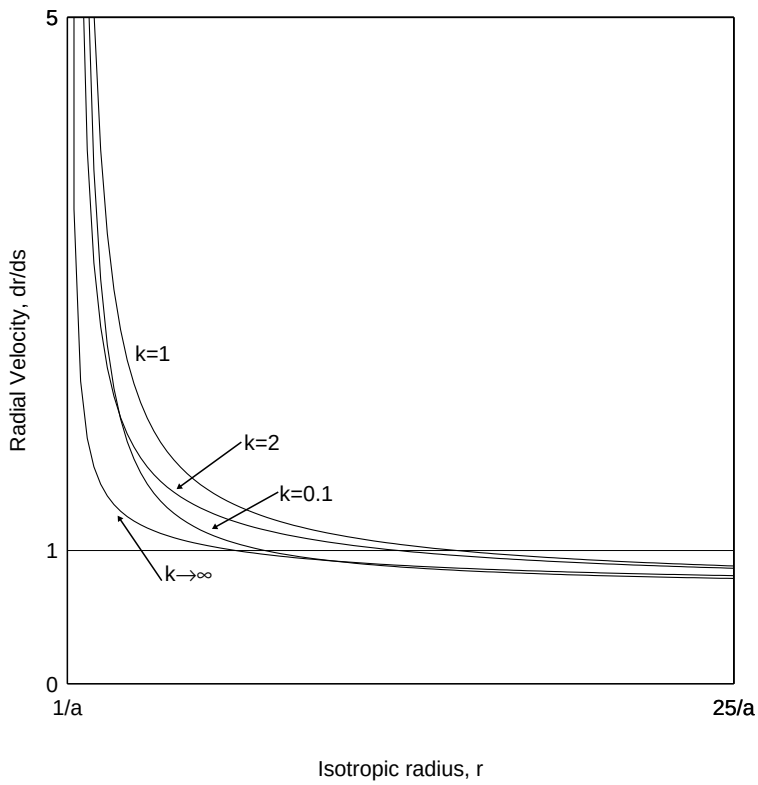

Figure 2.3: Radial velocity of particle as a function of isotropic r

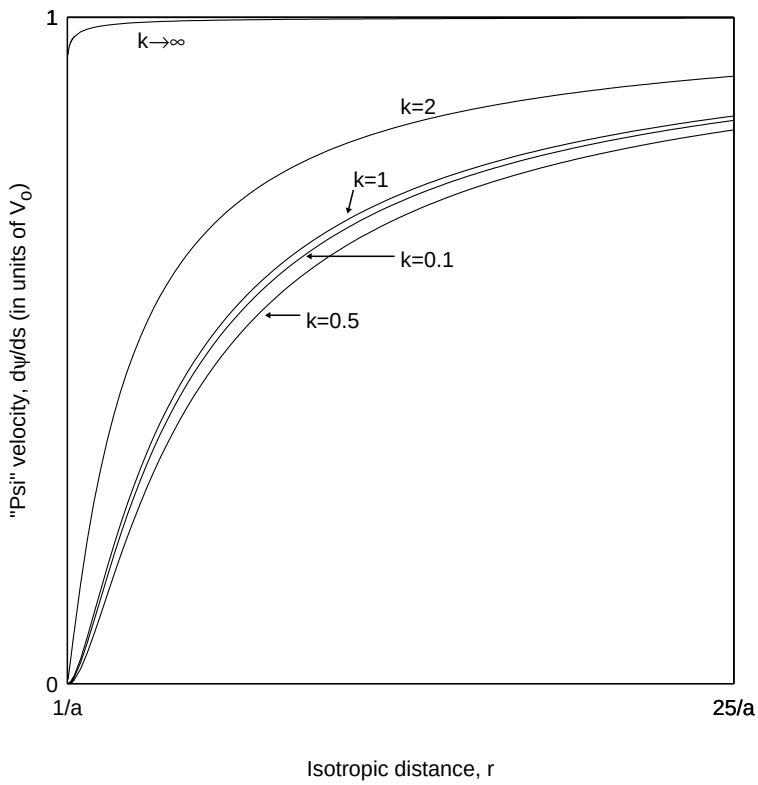

Figure 2.4: "Psi" velocity, $\dot{\psi}$, as a function of isotropic r

difference between perihelion shift in orbits between 4-D general relativity and these solitons [17, 21], it does not. The reason is simply that those results are obtained by looking at $du/d\phi$, where $u \equiv 1/r$; under the transformation (2.5) $\dot{\theta}$ and $\dot{\phi}$ may look the same as the 4-D case, but $\dot{r}$, $\dot{t}$ and $\dot{\psi}$ certainly do not take the same form as their 4-D counterparts.

The "psi" velocity starts initially at V_0 at radial infinity and slows to zero as it approaches the origin for as long as there is the slightest curvature in the fifth dimension. Only in the Schwarzschild limit, does this velocity remain constant for all r. The proper size of the fifth dimension itself remains finite near the origin. To see this, we write $d\psi_{prop} = C(r)d\psi$ and use $d\psi = \frac{d\psi}{ds}\frac{ds}{dr}dr = \left(\dot{\psi}/\dot{r}\right)dr$. Hence,

$$\begin{aligned} \psi_{prop} &= \int C\frac{V_0}{C^2\dot{r}}dr + \psi_o \\ \psi_{prop} &= \int \frac{V_0\ dr}{\sqrt{\frac{E^2C^2}{A^2B^2} - \frac{WL^2C^2}{B^4r^2} - \frac{V_0^2}{B^2} - \frac{\Xi C^2}{B^2}}} + \psi_o, \end{aligned} \tag{2.18}$$

where $r \geq 1/a$ by the above arguments. This is not analytically solvable for all (ϵ, κ), but can be iteratively computed. To do so, the size of ψ_{prop} is arbitrarily assumed at a given r (say $r = 1/a$). Since $(A, B, C) \rightarrow (0, 0, \infty)$ as $r \rightarrow \frac{1}{a}$, it is easy to see that $\psi_{prop}(r = \frac{1}{a}) = \psi_o$. The minimal size of the fifth dimension is then determined by the size of the integration constant ψ_o. **Figure 2.5** depicts ψ_{prop}

as a function of proper distance, $R_{prop} = \int_{1/a}^{r} B(r)dr$ which is also iteratively calculated ($R_{prop}(r=\frac{1}{a}) = 0$, $\psi_o = 0$, $\Xi = 1$, L=0, E=1.25 and V_0=0.25).

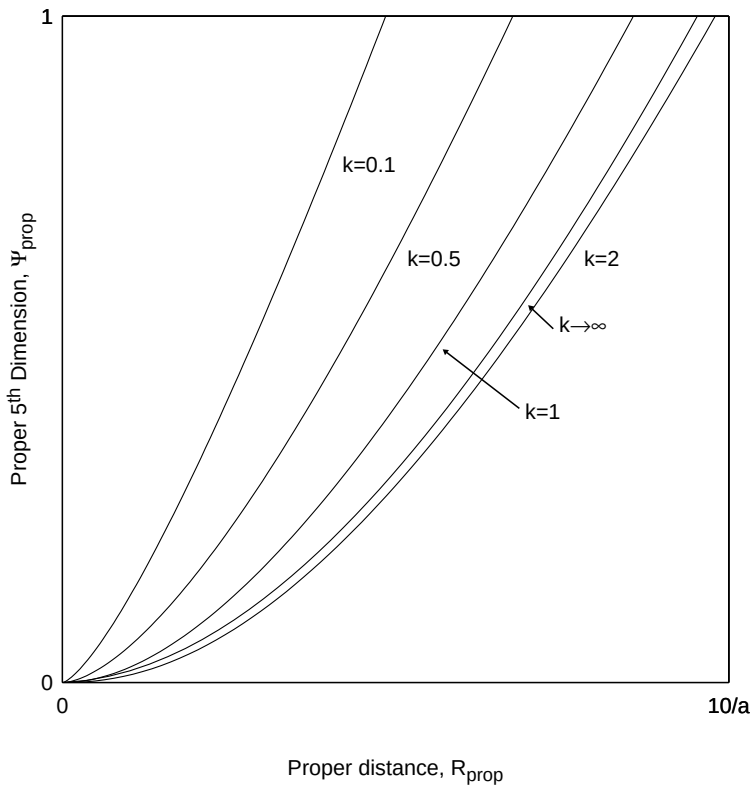

Figure 2.5: Proper size of fifth dimension for a radially travelling particle, ψ_{prop}, as a function of proper distance, R_{prop}

2.3 Stability of Circular Orbits

For simplicity, we will employ the transformation (2.5) in the limit $(\epsilon, \kappa, \epsilon\kappa) \rightarrow (0, \infty, 1)$, namely $\tilde{r} = r\left(1 + \frac{1}{ar}\right)^2$, for all (ϵ, κ) and use $a = \frac{2}{M}$. Since $0 \leq r < \infty$

covers $\tilde{r} \geq 2M$ twice by this transformation, then we will only consider circular orbits with $\tilde{r} \geq 2M$. Under this transformation, (2.1) will take the form

$$ds^2 = A^{\epsilon\kappa}dt^2 - A^{-\epsilon(\kappa-1)}d\tilde{r}^2 - A^{1-\epsilon(\kappa-1)}\tilde{r}^2 d\Omega^2 - A^{-\epsilon}d\psi^2,$$

with

$$A \equiv 1 - \frac{2M}{\tilde{r}},$$

and equation (2.14) now has the form ($\theta = \pi/2, \dot{\theta} = 0$)

$$\begin{aligned} \dot{\tilde{r}}^2 &+ A^{\epsilon(\kappa-1)}\Xi + A^{\epsilon\kappa}V_0^2 + A^{2\epsilon(\kappa-1)-1}\frac{L^2}{\tilde{r}^2} - A^{-\epsilon}E^2 = 0 \\ \dot{\tilde{r}}^2 &+ f(\tilde{r}) = 0. \end{aligned} \tag{2.19}$$

To have circular orbits, both $\dot{\tilde{r}}$ and $\ddot{\tilde{r}}$ must vanish at some radius, $\tilde{r} = \tilde{r}_*$, which corresponds to $f(\tilde{r})|_{\tilde{r}_*} = 0$ and $f'(\tilde{r})|_{\tilde{r}_*} = 0$, where a prime now denotes $\partial/\partial\tilde{r}$. Setting $f(\tilde{r}) = 0$, we obtain

$$E^2 = A^{\epsilon\kappa}\Xi + A^{\epsilon(\kappa+1)}V_0^2 + A^{\epsilon(2\kappa-1)-1}\frac{L^2}{\tilde{r}^2}, \tag{2.20}$$

which can then be substituted into $f'(\tilde{r})$ to yield

$$\begin{aligned} \tilde{f}'(\tilde{r}) &= \frac{\tilde{r}^2}{2M}A^{1-\epsilon\kappa}f'(\tilde{r}) \\ &= \epsilon\kappa A^{-\epsilon}\Xi + \epsilon(\kappa+1)V_0^2 + A^{\epsilon(\kappa-2)-1}\frac{L^2}{\tilde{r}^2}[\epsilon(2\kappa-1) + 1 - \tilde{r}/M] \end{aligned} \tag{2.21}$$

Setting (2.21) to zero yields the radius for circular orbits, $\tilde{r} = \tilde{r}_*$, which can then be substituted into (2.20) to give $E = E(\Xi, V_0, L)$.

To check to see if the orbit is stable or unstable at $\tilde{r} = \tilde{r}_*$, a particle is perturbed radially from $\tilde{r}_*$ by some small amount, $\tilde{r} = \tilde{r}_* + \delta$. Assuming $\delta \ll \tilde{r}_*$ so that $\mathcal{O}(\delta^3)$ terms are insignificant, (2.19) becomes

$$\dot{\delta}^2 + \frac{1}{2} f''(\tilde{r}_*)\delta^2 = 0, \tag{2.22}$$

and so a stable orbit exists at $\tilde{r}_*$ if $f''(\tilde{r}_*) > 0$ since (2.22) would represent oscillations with angular frequency $\sqrt{f''(\tilde{r}_*)/2}$. Similarly, if $f''(\tilde{r}_*) < 0$ then (2.22) will be an exponential growth/decay and thus there will be an unstable orbit at $\tilde{r}_*$.

Solving $f'(\tilde{r}) = 0$ (or $\tilde{f}'(\tilde{r}) = 0$) for $\tilde{r}$ in (2.21) is not analytically solvable for all values of κ (and ϵ), so finding radii of circular orbits for all values is not possible. However, it is possible to analytically solve for four cases: massless particles ($\Xi = 0$) with $V_0 = 0$, the Schwarzschild limit ($\kappa = \infty$), the Chatterjee case ($\kappa = 1$) and the "synchronous" case ($\kappa = 0$). These four cases will be studied in sections 2.3.1 to 2.3.4. Although one cannot solve for $\tilde{r}_*$ and $E(\Xi, V_0, L)$ for all κ, it is possible to infer the behavior of orbits in terms of stability for all κ. Therefore, sections 2.3.5 and 2.3.6 are devoted to looking at the behavior of

orbits for $1 < \kappa < \infty$ and $0 < \kappa < 1$, respectively.

2.3.1 Massless particles ($\Xi = 0$) with $V_0 = 0$ for all (ϵ, κ)

Solving $\tilde{f}'(\tilde{r}) = 0$ for $\tilde{r}$ in (2.21) and then simplifying (2.20) yields

$$\tilde{r}_* = [\epsilon(2\kappa - 1) + 1]M \equiv \tilde{r}_0, \tag{2.23}$$

$$E^2 = \frac{L^2/M^2}{[\epsilon(2\kappa - 1) + 1]^2} \left[\frac{\epsilon(2\kappa - 1) - 1}{\epsilon(2\kappa - 1) + 1}\right]^{\epsilon(2\kappa-1)-1}, \tag{2.24}$$

which agrees with previous work [17], and the general relativistic value of $\tilde{r}_* = 3M$ is retrieved in the Schwarzschild limit. For stability, we find that

$$f''(\tilde{r}_*) = -2\left(1 - \frac{2M}{\tilde{r}_*}\right)^{2[\epsilon(\kappa-1)-1]} \frac{L^2}{\tilde{r}_*^4} < 0,$$

and so all these orbits are unstable.

Since the manifold ends at $\tilde{r} = 2M$, the massless particles with $V_0 = 0$ can only have circular orbits for $\kappa > 1$. It is apparent in sections 2.3.3 and 2.3.4 that massless particles must have some sort of momentum in the fifth dimension, $V_0 \neq 0$, in order to have circular orbits for $\kappa \leq 1$.

2.3.2 Schwarzschild limit $(\epsilon, \kappa) = (0, \infty)$

There are two solutions in this limit,

$$\tilde{r}_*^{\pm} = \frac{L^2}{2M(\Xi + V_0^2)} \left(1 \pm \sqrt{1 - \frac{12M^2(\Xi + V_0^2)}{L^2}} \right),$$

which is identical to the general relativity value for $\Xi = 1$ and $V_0 = 0$. Like the 4-D Schwarzschild solution, there is a lower limit to the radii of circular orbits, which is here imposed by $L^2 > 12M^2(\Xi + V_0^2)$. Unlike the 4-D solution, however, massless particles can have circular orbits at radii other than $\tilde{r}_* = 3M$. The fact that $L^2 > M^2(\Xi + V_0^2)$ imposes a lower limit to L or an upper limit to V_0. For any given L, if V_0 is too large then no circular orbits will exist.

Letting $L^2 = 12nM^2(\Xi + V_0^2)$ with $n \in (1, \infty)$, we can parameterize the radii for circular orbits and the respective energies in terms of n:

$$\begin{aligned} \tilde{r}_*^{\pm} &= 6Mn\zeta & (2.25) \\ E_{\pm}^2 &= (\Xi + V_0^2) \left\{ 1 - \left[3n\zeta^2 \right]^{-1} + 2 \left[9n^2\zeta^3 \right]^{-1} \right\} \\ &= \frac{L^2}{12nM^2} \left\{ 1 - \left[3n\zeta^2 \right]^{-1} + 2 \left[9n^2\zeta^3 \right]^{-1} \right\}, & (2.26) \\ \zeta &= 1 \pm \sqrt{1 - \frac{1}{n}}. \end{aligned}$$

The two radii have the ranges $3M < \tilde{r}_*^- < 6M$ and $\tilde{r}_*^+ > 6M$. For stability,

we find that

$$f''(\tilde{r}_*) = \frac{2L^2}{\tilde{r}_*^5}\left(\tilde{r}_* - 6M\right),$$

and so $\tilde{r}_*^-$ represents unstable orbits and $\tilde{r}_*^+$ represents stable orbits. Hence, for $V_0 \neq 0$ it is possible for massless particles to have stable circular orbits for $\tilde{r} > 6M$ and unstable orbits not just at $\tilde{r} = 3M$ as with the 4-D solution.

2.3.3 Chatterjee case $(\epsilon, \kappa) = (1, 1)$

The Chatterjee solution is interesting since it sometimes yields the same results as the Schwarzschild limit because $\epsilon\kappa = 1$ for both cases. For example, the energy, $\dot{t}$, is identical in both cases, as well as the gravitational mass [22]. However, circular orbits are very much different between the two cases as will now be demonstrated. The radii and energies of circular orbits in the Chatterjee vacuum are

$$\tilde{r}_* = M\frac{4V_0^2 + L^2/M^2}{\Xi + 2V_0^2} \tag{2.27}$$

$$E^2 = \frac{L^2/M^2(V_0^2 + \Xi) - \Xi}{L^2/M^2 + 4V_0^2} \tag{2.28}$$

The orbits are all stable providing that $L^2/M^2 > 2\Xi$, which is derived from

$$f''(\tilde{r}_*) = \frac{2}{M^2}\frac{(\Xi + 2V_0^2)^4}{\left(4V_0^2 + L^2/M^2\right)^2\left(L^2/M^2 - 2\Xi\right)}.$$

With this limit on L, it is easy to see that $\tilde{r}_* > 2M$. One difference then between the Chatterjee case and the Schwarzschild limit is that the Chatterjee case has no unstable circular orbits. Another difference is that the radii of the stable orbits range the entire manifold except the origin. Furthermore, unlike the Schwarzschild limit, V_0 is not limited in its range; there is no value of L^2/M^2 over which the value of V_0^2 will destroy the possibility of circular orbits.

2.3.4 "Synchronous" case $(\epsilon, \kappa) = (1, 0)$

This limit has been coined "synchronous" here because an observer's time, t, differs from proper time, s, only by a constant factor (E), and $g_{tt} = 1$. As shown in section 2.3.1, there are no circular orbits for massless particles with $V_0 = 0$ for this case; if there were, they would exist at $\tilde{r}_* = 0$ which is not part of the 5-D manifold. However, for massive particles ($\Xi = 1$) or massless particles with $V_0 \neq 0$, we find

$$\tilde{r}_* = T_2^{\frac{1}{3}} - T_3 + \frac{1}{3}T_1 \tag{2.29}$$

$$E^2 = L^2 \frac{1 + \tilde{r}_*/M}{(\tilde{r}_* - 2M)^2} + \Xi, \tag{2.30}$$

where

$$
\begin{aligned}
T_1 &= 2M\left(\frac{1}{2}\tilde{L}^2+3\right) \\
T_2 &= 8M^3\left[\left(\frac{1}{6}\tilde{L}^2+1\right)^3-\left(\frac{1}{4}\tilde{L}^2+1\right)+\frac{1}{4}\tilde{L}^2\sqrt{1+\frac{2}{27}\tilde{L}^2}\right] \\
T_3 &= -\frac{4M^2}{T_2^{\frac{1}{3}}}\left[\frac{1}{6}\tilde{L}^2\left(\frac{1}{6}\tilde{L}^2+2\right)\right] \\
\tilde{L} &= \frac{L}{V_0 M}.
\end{aligned}
$$

As $\tilde{L} \to 0$ ($L \to 0$ or $V_0 \to \infty$) it may be verified that $\tilde{r}_* \to 2M$. Furthermore, as $\tilde{L} \to \infty$ ($L \to \infty$ or $V_0 \to 0$) then $\tilde{r}_* \to \infty$. If $V_0 = L/M$ then $\tilde{r} \approx 4.875M$. The condition for stability for this solution is

$$
f''(\tilde{r}_*) = \frac{2ML^2}{(\tilde{r}_*-2M)^5}\left[\frac{\tilde{r}_*}{M}+4\right] > 0,
$$

and therefore stable orbits are attainable for massless and massive particles at any radii in the manifold except at the origin. For this reason, and also for the fact that neither solutions have unstable circular orbits, the Chatterjee case and the "synchronous" case are very similar. Unlike the Chatterjee case, though, the radius of circular orbit here does not depend on the particle being massive or massless.

2.3.5 Circular Orbits for $1 < \kappa < \infty$

For this range in κ, we note that $2 < [x \equiv \epsilon(2\kappa - 1) + 1] < 3$, $-2 < [\omega \equiv \epsilon(\kappa - 2) - 1] < 0$ and $0 < \epsilon < 1$, and thus equation (2.21) becomes

$$\begin{aligned} \tilde{f}'(\tilde{r}) &= \epsilon(\kappa+1)V_0^2 + F_1 + F_2 \\ F_1 &= \frac{\epsilon\kappa\Xi}{(1-2M/\tilde{r})^{\epsilon}} \\ F_2 &= \frac{L^2\,(x-\tilde{r}/M)}{\tilde{r}^2\,(1-2M/\tilde{r})^{|\omega|}} \end{aligned}$$

Now, $\epsilon(\kappa+1)V_0^2$ and F_1 are both positive for all $\tilde{r} > 2M$. As $\tilde{r} \to 2M$, $F_2 \to +\infty$ since $x > 2$, but $F_2 \to 0^-$ as $\tilde{r} \to \infty$; that is, F_2 has one zero at $\tilde{r} = xM\tilde{r}_0$, which agrees with results in section 2.3.1 for $\Xi = 0$ and $V_0 = 0$. Furthermore, F_2 has a minimum at $\tilde{r} = \tilde{r}_1 \equiv [3\epsilon(\kappa-1)+1+\sqrt{4-3\epsilon^2\kappa}]M$, which has the range $2M < \tilde{r}_1 < 6M$ for $k > 1$. Also, $F_2'|_{\tilde{r}<\tilde{r}_1} < 0$ and $F_2'|_{\tilde{r}>\tilde{r}_1} > 0$. **Figure 2.6** depicts the general shape of F_2 (for all κ), although the width, depth and location of the "well" will vary according to the values of L and κ.

If $V_0 \neq 0$ or $\Xi = 1$ it is easy to see that $\tilde{f}'(\tilde{r}) \to 0^+$ as $\tilde{r} \to \infty$. Providing that V_0 is not too large, or L^2 is not too small, there will be two zeroes for $\tilde{f}'(\tilde{r})$. The zero closest to the origin corresponds to the zero of F_2, but shifted to higher $\tilde{r}$, and gives the radius for an unstable orbit, $\tilde{r}_*^-$, since both $F_2'|_{\tilde{r}<\tilde{r}_1} < 0$ and $F_1'|_{\tilde{r}>2M} < 0$. The second zero is at the radius of a stable orbit, $\tilde{r}_*^+$, since

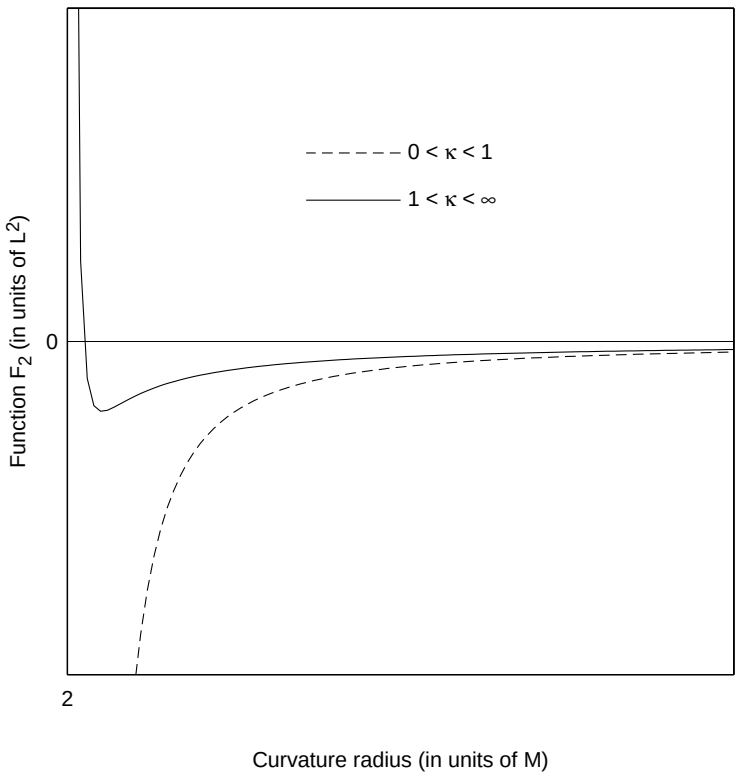

Figure 2.6: General form of F_2, or $\tilde{f}'(\tilde{r})$ with $\Xi = 0$ and $V_0 = 0$.

$F_2'|_{\tilde{r}>\tilde{r}_1} > 0$ and $|F_2'| > |F_1'|$ for $\tilde{r} > \tilde{r}_1$ because $|\omega| > \epsilon$.

If V_0 is too large, then $\tilde{f}'(\tilde{r}) > 0$ for all $\tilde{r} > 2M$ and there will be no circular orbits. Therefore, V_0 has an upper limit $V_{0(max)}$. Similarly, if L is too small when either $V_0 \neq 0$ or $\Xi = 1$, no orbits will exist either, giving a lower limit to L, $L_{(min)}$. However, $V_{0(max)}$ and $L_{(min)}$ depend on ϵ, κ and Ξ, as well as each other, and may not necessarily be found analytically for all κ.

Suppose $V_0 = 0$ and $\Xi = 1$, and $L = L_{(min)}$ such that the minimum of $\tilde{f}'(\tilde{r})$

corresponds to $\tilde{f}'(\tilde{r}) = 0$. In this case there would only be one circular orbit, the radius and $L_{(min)}$ of which would be

$$\begin{aligned} \tilde{r} &= \tilde{r}_2 \equiv \left[\epsilon(3\kappa - 2) + 1 + \sqrt{3\epsilon^2\kappa^2 - 4\epsilon^2\kappa + 1}\right] M \\ L^2_{(min)} &= \frac{\epsilon\kappa(\tilde{r}_2/M)^{\epsilon(\kappa-1)+1}(\tilde{r}_2/M - 2)^{1-\epsilon(\kappa-1)}}{\epsilon(\kappa - 1) + \sqrt{3\epsilon^2\kappa^2 - 4\epsilon^2\kappa + 1}} M^2, \end{aligned}$$

which have ranges $2M < \tilde{r}_2 < 6M$ and $2M^2 < L^2 < 12M^2$ for $1 < \kappa < \infty$. As L gets larger the minimum of $\tilde{f}'(\tilde{r})$ will become negative and there will again be two radii of circular orbits, $\tilde{r}_*^+ > \tilde{r}_2$ and $xM < \tilde{r}_*^- < \tilde{r}_2$.

If $\Xi = 0$, we'd see that for $V^2_{0(max)}$, a unique circular orbit will lie at $\tilde{r} = \tilde{r}_1$ and

$$L^2 = \epsilon(\kappa + 1)V^2_{0(max)} \frac{(\tilde{r}_1/M)^{\epsilon(\kappa-2)+1}(\tilde{r}_1/M - 2)^{1-\epsilon(\kappa-2)}}{\epsilon(\kappa - 2) + \sqrt{4 - 3\epsilon^2\kappa}} M^2,$$

with the range $0 < L^2 < 12M^2V^2_{0(max)}$ for this range in κ. Again, upon increasing L or decreasing V_0, stable orbits would exist at $\tilde{r}_*^+ > \tilde{r}_1$, and unstable orbits at $\tilde{r}_0 < \tilde{r}_*^- < \tilde{r}_1$.

If $V_0 \neq 0$ and $\Xi = 1$, then when $\tilde{f}'(\tilde{r}) = 0$ is at the minimum of $\tilde{f}'(\tilde{r})$, the only circular orbit will lie at some $\tilde{r}$ between $\tilde{r}_1$ and $\tilde{r}_2$ since the latter is greater than the former. Stable orbits will exist at radii greater than this radius and unstable orbits between this radius and $\tilde{r} = xM$.

To generalize, for $1 < \kappa < \infty$ there are two radii for circular orbits. The inner

radius (unstable orbit) may only be as small as $\tilde{r} = xM$, whilst the outer radius (stable orbit) has a lower limit somewhere between $\tilde{r}_1$ and $\tilde{r}_2$, depending on Ξ, V_0 and L. Furthermore, by setting V_0^2 too high, or L^2 too low, then $\tilde{f}'(\tilde{r}) > 0$ for all $\tilde{r} > 2M$ and no circular orbits will exist. Thus, all solitons with $1 < \kappa < \infty$ behave similarly to the Schwarzschild case for circular orbits.

2.3.6 Circular Orbits for $0 < \kappa < 1$

For this range in κ, we find that $0 < [x \equiv \epsilon(2\kappa - 1) + 1] < 2$ so that $Mx - \tilde{r} < 0$, $-3 < [\omega \equiv \epsilon(\kappa - 2) - 1] < -2$ and $1 < \epsilon < 2/\sqrt{3}$, and so equation (2.21) will look like

$$\tilde{f}'(\tilde{r}) = \epsilon(\kappa + 1)V_0^2 + \frac{\epsilon\kappa\Xi}{(1 - 2M/r)^{\epsilon}} - \frac{L^2 \left|x - \tilde{r}/M\right|}{\tilde{r}^2 \left(1 - 2M/r\right)^{|\omega|}}$$

Now, $\tilde{f}'(\tilde{r}) \to -\infty$ as $\tilde{r} \to 2M$ since $|\omega| > \epsilon$. Furthermore, $f''(\tilde{r}) > 0$ for all $\tilde{r} > 2M$ since the L^2 term is the most dominant term for both $\tilde{r} \to 2M$ and $\tilde{r} \to \infty$.

If $\Xi = 0$ and $V_0 = 0$ then $\tilde{f}'(\tilde{r}) \to 0^-$ as $\tilde{r} \to \infty$ (see **figure 2.6**) and will never therefore be zero. Hence, no circular orbits will exist. If $\Xi = 1$ or $V_0 \neq 0$, then $\tilde{f}'(\tilde{r}) \to 0^+$ as $\tilde{r} \to \infty$ and so $\tilde{f}'(\tilde{r})$ will have one zero corresponding

to a radius having a stable circular orbit. Hence, like the Chatterjee case and the "synchronous" case, there are no circular orbits for massless particles with $V_0 = 0$; otherwise there are stable circular orbits for all $\tilde{r} > 2M$. In this range of κ, V_0 has no upper bound limiting circular orbits; as V_0 gets larger, the radii for circular orbits approaches $r_* = 2M$.

Chapter 3

Isotrope Solutions

3.1 Static, Inhomogeneous Isothermal Solutions

We next seek to find a five-dimensional analogue to the four-dimensional static, inhomogeneous isothermal solutions that was developed by Henriksen and Wesson [23, 24], described by the line interval

$$ds^2 \;=\; r^{\frac{4p_o}{p_o+\eta_o}}dt^2 \;-\; \frac{dr^2}{1-\eta_o} \;-\; r^2 d\Omega^2. \tag{3.1}$$

The density and pressure of the fluid described by (3.1) is, respectively, $\rho = \eta_o/r^2$ and $p = p_o/r^2$, and to ensure that the fluid remains static ($\ddot{r} = 0$) there is a consistency relationship between η_o and p_o: $4p_o(1-\eta_o) = (p_o+\eta_o)^2$. For physical reasons, the parameter η_o is limited to $0 \leq \eta_o \leq \frac{1}{2}$ which then limits

p_o to $0 \leq p_o \leq \frac{1}{2}$. This solution has astrophysical importance since the density and pressure relationships above are those approached by many rich clusters of galaxies.

In the induced matter scenario, it would be useful to find a five-dimensional analogue which would appear to be a vacuum in five dimensions, but would give a fluid of pressure and density proportional to r^{-2} in four dimensions. Furthermore, it has been previously shown [9] that in the induced matter theory, any metric that is solely dependent on the radial co-ordinate will only produce a radiation equation of state, $\rho = 3p$. Therefore, in order to obtain a class of solutions with equations of state other than radiation, the metric must be dependent on the extra coordinate, ψ (the metric could also depend on the time coordinate, t, but the fluid here should be static and hence independent of time). Thus, the five-dimensional metric found that satisfies these criteria is

$$\begin{aligned} ds^2 &= \left(\frac{r}{r_o}\right)^{2(\alpha+1)} \psi^{2(1+3/\alpha)} dt^2 \; - \; (3-\alpha^2)\, \psi^2 dr^2 \; - \; r^2 \psi^2\, d\Omega^2 \\ &\quad + \frac{3}{\alpha^2}(3-\alpha^2)\, r^2 d\psi^2, \end{aligned} \tag{3.2}$$

which, on hypersurfaces of ψ, can be made to look similar to (3.1). From dimensional arguments, if we say that r has units of length, then ψ must be

unitless (i.e. multiplied by the appropriate constants to be unitless). Hence, the constant $r_o^{2(\alpha+1)}$ is placed in the dt^2 term to render g_{tt} unitless. We could have easily written $r_o = 8\pi GM/c^2 \equiv M$ where M is a constant with units of mass. This "juggling" of units is useful later in this section when the induced gravitational mass is calculated.

In general, if we write $g_{44} = g_{\psi\psi} = \epsilon\Phi^2$, where $\epsilon = \pm 1$, and assume $g_{\alpha 4} = 0$ then the effective energy-momentum tensor is [9]

$$\begin{aligned} T_{\alpha\beta} &= \frac{\Phi_{\alpha;\beta}}{\Phi} - \frac{\epsilon}{2\Phi^2}\left\{\frac{\overset{*}{\Phi}\overset{*}{g}_{\alpha\beta}}{\Phi} - \overset{**}{g}_{\alpha\beta} + g^{\mu\nu}\,\overset{*}{g}_{\alpha\mu}\overset{*}{g}_{\beta\nu}\right. \\ &\quad \left. -\frac{g^{\mu\nu}\,\overset{*}{g}_{\mu\nu}\overset{*}{g}_{\alpha\beta}}{2} + \frac{g_{\alpha\beta}}{4}\left[\overset{*}{g}{}^{\mu\nu}\overset{*}{g}_{\mu\nu} + \left(g^{\mu\nu}\,\overset{*}{g}_{\mu\nu}\right)^2\right]\right\}. \end{aligned} \tag{3.3}$$

The semi-colon represents the usual (3+1) covariant derivative, $\Phi_\alpha = \partial\Phi/\partial x^\alpha$ and an overstar represents $\partial/\partial\psi$.

For (3.2) the four non-zero components of (3.3) in mixed form (i.e. T^α_β) are

$$\begin{aligned} T^t_t &= \frac{2-\alpha^2}{(3-\alpha^2)\psi^2 r^2} \\ T^r_r &= -\frac{\alpha(\alpha+2)}{(3-\alpha^2)\psi^2 r^2} \\ T^\theta_\theta &= -\frac{(\alpha+1)^2}{(3-\alpha^2)\psi^2 r^2} \end{aligned}$$

$$T^{\phi}_{\phi} = T^{\theta}_{\theta}. \tag{3.4}$$

Using the convention used in [19], we associate the density with T^t_t and the pressure with $-\frac{1}{3}(T^r_r + T^\theta_\theta + T^\phi_\phi)$ to yield

$$\rho = \frac{2-\alpha^2}{(3-\alpha^2)\psi^2 r^2} \tag{3.5}$$

$$p = \frac{\alpha^2 + 2\alpha + 2/3}{(3-\alpha^2)\psi^2 r^2}. \tag{3.6}$$

From whence it follows that we have an isothermal equation of state, $p = (\alpha^2 + 2\alpha + 2/3)/(2-\alpha^2)\ \rho$.

Figure 3.1 clearly illustrates how these istropes differ from their 4-D counterparts in several ways. First, because of the consistency relationship with p_o and η_o in (3.1), the pressure and density in the (3+1) theory are always positive. For (3.5) and (3.6), ρ remains positive for $-\sqrt{2} < \alpha < \sqrt{2}$ (which physically restricts α), but p is negative for $\alpha < -1 + 1/\sqrt{3} \approx -0.42$. Hence, the five-dimensional case is richer in that it involves many more equations of state, including that of dust, $p = 0$ with $\rho \neq 0$. For (3.1), $p = 0$ only when $\rho = 0$ and the metric is flat and devoid of matter. For $\alpha^2 \leq 2$, we find other equations of state, such as radiation ($\rho = 3p$) at $\alpha = 0$, stiff ($\rho = p$) at $\alpha = \sqrt{\frac{11}{12}} - \frac{1}{2} \approx 0.46$ and vacuum ($\rho = -p$) at $\alpha = -\frac{4}{3}$. However, we will now show that $\alpha > -1$ which then excludes the vacuum solution.

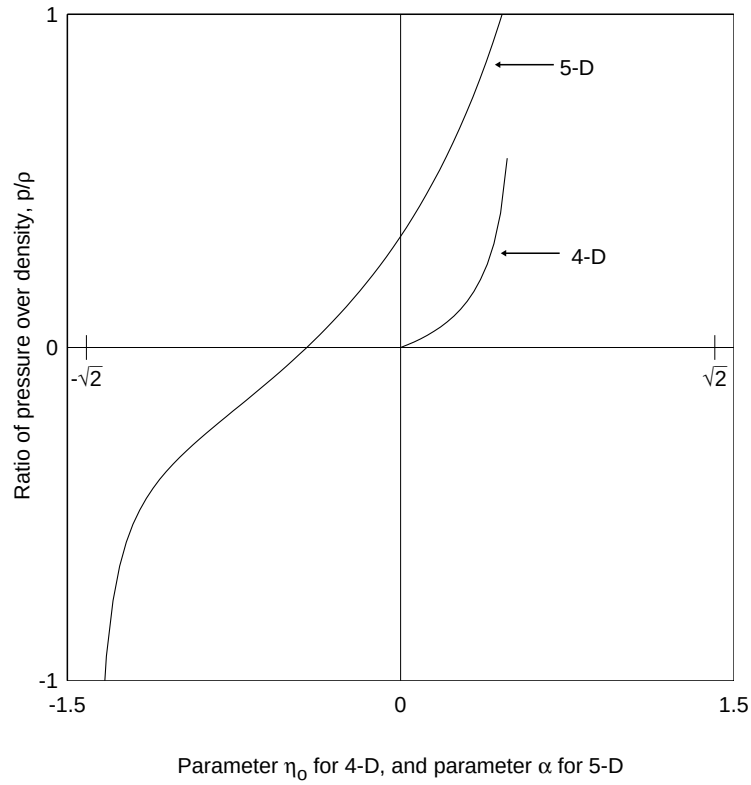

Figure 3.1: Ratio of pressure to density, p/ρ, for 4-D and 5-D models.

We can calculate the gravitational mass of the fluid, M_g, using the standard (3+1) definition [25, 26]:

$$\begin{aligned} M_g(r,\psi) &\equiv \int (T_0^0 - T_1^1 - T_2^2 - T_3^3)\sqrt{-g_4}\, dV_3 \\ &= \frac{8\pi(\alpha+1)}{\sqrt{3-\alpha^2}}\psi^{2+3/\alpha}\left(\frac{r}{r_o}\right)^{2+\alpha} r_o, \end{aligned} \tag{3.7}$$

where g_4 is the determinant of the four-dimensional part of the metric. If we were to restore full units, then the last constant in (3.7) would read $\frac{c^2 r_o}{8\pi G}$ which

has units of mass (again, we could write $\frac{c^2 r_o}{8\pi G} = M$). The 4-D mass defined in [23] differs from (3.7) since the former's dependence on radial distance is strictly linear. However, their definition of mass was different from (3.7). Applying the definition in (3.7) to (3.1), one would obtain

$$^{(4)}M_g(r) \;=\; 8\pi\sqrt{p_o}\; r^{\left(\frac{2p_o}{p_o+\eta_o}+1\right)},$$

which is then analogous to (3.7).

It is apparent from (3.7) that $\alpha \geq -1$ in order that the mass remains positive. Therefore equations of state $p < -\rho/3$ are not permitted in these solutions. The radiation solution must be ruled out as well, since there is a divergence in the metric when $\alpha = 0$. However, this would appear to be an artifact since invariants such as the Kretschmann scalar,

$$R^{abcd}R_{abcd} = \frac{16}{3\psi^4 r^4}, \tag{3.8}$$

reveal no singularity at $\alpha = 0$, although they are not well behaved at $\psi = 0$ and $r = 0$. However, although the density and pressure are well behaved at $\alpha = 0$ it is evident that the gravitational mass may diverge. As $\alpha \to 0^-$, $M_g \to 0$ for $\psi > 1$, but diverges for $\psi < 1$. Conversely, as $\alpha \to 0^+$, $M_g \to 0$ for $\psi < 1$, but diverges for $\psi > 1$. So, it is possible to infer the behavior of M_g as the

radiation equation is *approached*, but $\alpha = 0$ must remain an unphysical case in this solution. This is not too severe of a restriction since (3.2) is being used to describe systems such as clusters of galaxies which are not generally described by a radiation equation of state.

3.2 Geodesic Motion

The motion of a particle in a manifold described by (3.2) is governed by the five geodesic equations:

$$\ddot{t} = -2\frac{(\alpha+1)}{r}\dot{t}\dot{r} - 2\frac{(1+3/\alpha)}{\psi}\dot{t}\dot{\psi} \tag{3.9}$$

$$\begin{aligned}\ddot{r} &= -\frac{(\alpha+1)}{(3-\alpha^2)r\psi^2}\left(\frac{r}{r_o}\right)^{2(\alpha+1)}\psi^{2(1+3/a)}\,\dot{t}^2 + \frac{r}{3-\alpha^2}\left(\dot{\theta}^2+\sin^2\theta\dot{\phi}^2\right) \\ &\quad -2\frac{\dot{r}\dot{\psi}}{\psi} - \frac{3}{\alpha^2}\frac{r\dot{\psi}^2}{\psi^2}\end{aligned} \tag{3.10}$$

$$\ddot{\theta} = -2\frac{\dot{r}\dot{\theta}}{r} - 2\frac{\dot{\psi}\dot{\theta}}{\psi} + \sin\theta\cos\theta\dot{\phi}^2 \tag{3.11}$$

$$\ddot{\phi} = -2\frac{\dot{r}\dot{\phi}}{r} - 2\frac{\dot{\psi}\dot{\phi}}{\psi} - 2\frac{\cos\theta}{\sin\theta}\dot{\theta}\dot{\phi} \tag{3.12}$$

$$\begin{aligned}\ddot{\psi} &= \frac{\alpha^2}{3}\frac{(1+\alpha/3)}{(3-\alpha^2)r^2\psi}\left(\frac{r}{r_o}\right)^{2(\alpha+1)}\psi^{2(1+3/a)}\,\dot{t}^2 - \frac{\alpha^2}{3}\frac{\psi}{3-\alpha^2}\left(\dot{\theta}^2+\sin^2\theta\dot{\phi}^2\right) \\ &\quad -2\frac{\dot{r}\dot{\psi}}{r} - \frac{\alpha^2}{3}\frac{\psi\dot{r}^2}{r^2}\end{aligned} \tag{3.13}$$

where, again, an overdot represents d/ds, with s as a proper time for massive

particles and some other affine parameter for photons. Using similar Killing vector arguments as chapter 2, equations (3.9) and (3.12) are easy to solve to obtain $\dot{t}$ and $\dot{\phi}$. Similarly, $\dot{\theta}$ can be obtained using the exact same method as in chapter 2. The three velocities are hence,

$$\dot{t} = E\left(\frac{r}{r_o}\right)^{-2(1+\alpha)}\psi^{-2(1+3/\alpha)} \tag{3.14}$$

$$\dot{\theta} = \frac{L}{r^2\psi^2}\sqrt{W - \csc^2\theta} \tag{3.15}$$

$$\dot{\phi} = \frac{L}{r^2\psi^2\sin^2\theta}. \tag{3.16}$$

The constant L is associated with the angular momentum of the particle and E has units of energy (per unit rest mass for massive particles). Like the soliton solution, if the particle is in the $\theta = \pi/2$ plane with $\dot{\theta} = 0$, it will remain there, and so $W = 1$ in that instance. The energy of the particle, $\dot{t}$, does not depend on r for $\alpha = -1$, which corresponds to $M_g = 0$ in the induced matter picture, and decreases with increasing r for other values of α. This is consistent with the (3+1) solution where

$$^{(4)}\dot{t} = E\, r^{\frac{-4p_o}{p_o+\eta_o}}.$$

For $-1 \leq \alpha < 0$, $\dot{t}$ increases with increasing ψ, but decreases with increasing ψ for $0 < \alpha \leq \sqrt{2}$.

Solving for $\dot{r}$ and $\dot{\psi}$ is not quit so easy as the other velocities, although one can also use the equation

$$\Xi = g_{AB}\frac{dx^A}{ds}\frac{dx^B}{ds}, \tag{3.17}$$

which is obtained by dividing (3.2) by ds^2. One velocity is then obtained by solving either (3.10) or (3.13), and the other is directly obtained through (3.17) ($\Xi = 0$ for massless particles and $\Xi = 1$ for massive particles). Even so, it is difficult to solve for $\dot{r}$ and $\dot{\psi}$ in this co-ordinate system, and so it is more convenient to use the system

$$\begin{aligned} R &= \frac{\sqrt{3}}{2}\left\{C\psi^{(1+\sqrt{3}/\alpha)}\ r^{(1+\alpha/\sqrt{3})} + \frac{1}{C}\psi^{(1-\sqrt{3}/\alpha)}\ r^{(1-\alpha/\sqrt{3})}\right\} \\ \Psi &= \frac{\sqrt{3}}{2}\left\{C\psi^{(1+\sqrt{3}/\alpha)}\ r^{(1+\alpha/\sqrt{3})} - \frac{1}{C}\psi^{(1-\sqrt{3}/\alpha)}\ r^{(1-\alpha/\sqrt{3})}\right\}, \end{aligned} \tag{3.18}$$

where,

$$C = \left(\frac{\sqrt{3}-\alpha}{\sqrt{3}+\alpha}\right)^{\sqrt{3}}.$$

In this system, (3.2) becomes

$$ds^2 = \frac{A}{3C}(R+\Psi)^{1+\sqrt{3}}(R-\Psi)^{1-\sqrt{3}}\,dt^2 - dR^2 - \frac{R^2-\Psi^2}{3}\,d\Omega^2 + d\Psi^2, \tag{3.19}$$

where $A = r_o^{-2(1+\alpha)}$. Equations (3.14)-(3.16) become

$$\dot{t} = E\frac{3C}{A}(R+\Psi)^{-1-\sqrt{3}}(R-\Psi)^{-1+\sqrt{3}} \tag{3.20}$$

$$\dot{\theta} = \frac{3L}{R^2-\Psi^2}\sqrt{W-\csc^2\theta} \tag{3.21}$$

$$\dot{\phi} = \frac{3L}{R^2-\Psi^2}\csc^2\theta, \tag{3.22}$$

and equations (3.10), (3.13) and (3.17) are replaced with (after substitution with $\dot{t}$, $\dot{\theta}$ and $\dot{\phi}$),

$$\ddot{R} = -\frac{3C}{A}\frac{E^2\ (R-\sqrt{3}\Psi)}{(R+\Psi)^{2+\sqrt{3}}\ (R-\Psi)^{2-\sqrt{3}}} + \frac{3WL^2R}{(R^2-\Psi^2)^2} \tag{3.23}$$

$$\ddot{\Psi} = -\frac{3C}{A}\frac{E^2(\sqrt{3}R-\Psi)}{(R+\Psi)^{2+\sqrt{3}}\ (R-\Psi)^{2-\sqrt{3}}} + \frac{3WL^2\Psi}{(R^2-\Psi^2)^2} \tag{3.24}$$

$$\dot{R}^2 - \dot{\Psi}^2 = \frac{3C}{A}\frac{E^2}{(R+\Psi)^{1+\sqrt{3}}\ (R-\Psi)^{1-\sqrt{3}}} - \frac{3\,W\,L^2}{R^2-\Psi^2} - \Xi. \tag{3.25}$$

This system is better since there are no cross terms in the differential equations ((3.23) and (3.24)) as there were before. However, one further simplification can be made, which is to let $u = R+\Psi$ and $v = R-\Psi$. From this, the three equations to solve are

$$v\ddot{u} = -\frac{3C}{A}\frac{E^2\ (1-\sqrt{3})}{u^{1+\sqrt{3}}\ v^{1-\sqrt{3}}} + \frac{3WL^2}{uv} \tag{3.26}$$

$$u\ddot{v} = -\frac{3C}{A}\frac{E^2\ (1+\sqrt{3})}{u^{1+\sqrt{3}}\ v^{1-\sqrt{3}}} + \frac{3WL^2}{uv} \tag{3.27}$$

$$\dot{u}\dot{v} = \frac{3C}{A}\frac{E^2}{u^{1+\sqrt{3}}\ v^{1-\sqrt{3}}} - \frac{3WL^2}{uv} - \Xi. \tag{3.28}$$

Adding (3.26) and (3.27) and then substituting in (3.28) finally yields the result,

$$\begin{aligned} (uv)^{\cdot\cdot} &= -2\Xi \\ uv &= -\Xi\, s^2 \ + \ 2\, k_1\, s \ + \ k_2. \end{aligned} \tag{3.29}$$

Hence, the parameter s can be arranged in terms of uv and then $\dot{u}$ and $\dot{v}$ can then be found in terms of u and v. The inverse transformations can then be performed to obtain $\dot{r}$ and $\dot{\psi}$. A note should first be made about the nature of k_1 and k_2. It is easy to show that indeed $uv = 3r^2\psi^2$, and so $(uv)^{\cdot\cdot}$ is the same as $(3r^2\psi^2)^{\cdot\cdot}$, etc. Suppose a particle starts initially ($s = 0$) at r_i and ψ_i. Then from (3.29) it is apparent that $k_2 = 3r_i^2\psi_i^2$, i.e. three times the product of the initial squared positions in r and ψ. Similarly, k_1 is defined as $k_1 = \frac{3}{2}(r^2\psi^2)^{\cdot}_i = 3r_i\psi_i(r_i\dot{\psi}_i + \psi_i\dot{r}_i)$. For ease in notation, however, the two constants will be redefined, so the velocities can be written

$$\dot{r} = \frac{\pm 1}{(3-\alpha^2)r\psi^2}\left(\sqrt{B_1} + \frac{\alpha}{\sqrt{3}}\sqrt{B_2}\right) \tag{3.30}$$

$$\dot{\psi} = \frac{\mp\alpha}{\sqrt{3}(3-\alpha^2)r^2\psi}\left(\frac{\alpha}{\sqrt{3}}\sqrt{B_1}+\sqrt{B_2}\right), \tag{3.31}$$

where

$$B_1 = k_1^2 + \Xi\, k_2 - 3\Xi r^2\psi^2$$

$$B_2 = k_1^2 + \Xi\, k_2 - 3\, E^2\, r_o^2 \left(\frac{r}{r_o}\right)^{-2\alpha} \psi^{-6/\alpha} + 3\, W\, L^2.$$

Of course, the square roots limit where a particle can be in the manifold. In particular, a particle can be at position (r, ψ) in the manifold, only if the conditions

$$k_1^2 + \Xi k_2^2 \geq 3\Xi\, r^2\, \psi^2$$

$$k_1^2 + \Xi k_2^2 \geq 3\, E^2\, r_o^2 \left(\frac{r}{r_o}\right)^{-2\alpha} \psi^{-6/\alpha} - 3\, W\, L^2$$

are satisfied. The first condition is automatically satisfied for photons ($\Xi = 0$). The second condition implies two things. For $\alpha < 0$ a particle may start near the origin (with a very large velocity), but cannot escape to spatial infinity. For $\alpha > 0$ a particle may escape to infinity but cannot approach the origin. For $\alpha = 0$ the second condition is divergent due to the ψ term.

In future work, these solutions will be used in 5-D gravitational lens computations. Previously, such calculations were performed using the soliton metric [17] but this is a poor approximation to clusters of galaxies, and the isotrope

solution studied in this chapter is superior.

Chapter 4

Vacuum Waves

4.1 Cosmological Models from Flat Space-times

In this chapter all metrics are flat. However, various cosmological models can be obtained by performing co-ordinate transformations and then viewing the metric along hypersurfaces of $x^4 = constant$. Although the main focus here is to examine one particular solution which gives an equation of state for a vacuum, we will first briefly take a look at a class of solutions that have been studied in detail.

We begin with a five-dimensional, "Minkowski" metric,

$$ds^2 \;=\; dT^2 \;-\; (dR^2 \;+\; R^2\, d\Omega^2) \;-\; d\Psi^2.$$

Although the signature of the fifth co-ordinate is spacelike , it could easily be

timelike here. In the co-ordinate transformations to follow, Ψ would be replaced with $i\Psi$ if a timelike co-ordinate is preferred. However, in the metrics that follow, the signature of the extra co-ordinate shown is necessary for that metric (i.e. changing the signature would render the metric no longer flat). In some cases, the signature can be changed, but the physical meaning of the metric changes as well.

We first find that the transformation

$$\begin{aligned} T &= \frac{\alpha}{2}\left(t^{\frac{1}{\alpha}}\psi^{\frac{1}{1-\alpha}}\right)\left[1+\left(\frac{r}{\alpha}\right)^2\right] - \frac{\alpha}{2(1-2\alpha)}\left(t^{-1}\psi^{\frac{\alpha}{1-\alpha}}\right)^{\frac{1-2\alpha}{\alpha}} \\ \Psi &= \frac{\alpha}{2}\left(t^{\frac{1}{\alpha}}\psi^{\frac{1}{1-\alpha}}\right)\left[1-\left(\frac{r}{\alpha}\right)^2\right] + \frac{\alpha}{2(1-2\alpha)}\left(t^{-1}\psi^{\frac{\alpha}{1-\alpha}}\right)^{\frac{1-2\alpha}{\alpha}} \\ R &= r\,t^{\frac{1}{\alpha}}\,\psi^{\frac{1}{1-\alpha}} \end{aligned} \tag{4.1}$$

renders the "Minkowski" metric into the form

$$ds^2 \;=\; \psi^2\,dt^2 \;-\; t^{\frac{2}{\alpha}}\psi^{\frac{2}{1-\alpha}}\left(dr^2 \;+\; r^2\,d\Omega^2\right) - \alpha^2(1-\alpha)^{-2}\,t^2\,d\psi^2, \tag{4.2}$$

which has been studied in depth [28, 29]. In the induced matter theory, this metric describes a (3+1) fluid with density and pressure relations

$$\rho = \frac{3}{\alpha^2 t^2 \psi^2}, \qquad p = \frac{(2\alpha-3)}{\alpha^2 t^2 \psi^2}, \qquad p = \frac{(2\alpha-3)}{3}\rho. \tag{4.3}$$

On hypersurfaces $\psi = constant$, (4.2) reduces to the standard Friedmann-Robertson-Walker (FRW) metric with a flat 3-D spatial section and hence is

relevant cosmologically. For $\alpha = 2$, the fluid has an expansion factor proportional to $t^{\frac{1}{2}}$ and is descriptive of the early universe ($p = \rho/3$). For $\alpha = 3/2$, the expansion factor is proportional to $t^{\frac{2}{3}}$ and the metric is descriptive of the late universe ($p = 0$). However, the vacuum equation of state ($p = -\rho$) is not well described by this metric since $\alpha = 0$ leads to a divergence in the spatial component of (4.2).

To find a cosmological metric with such an equation of state, we once again return to the "Minkowski" metric and find that the transformation

$$\begin{aligned} T &= \frac{2\psi}{\omega}\left[\sin(\frac{1}{2}\omega t) \pm \frac{i\omega^2 r^2}{8} e^{\pm i\omega t/2}\right] \\ \Psi &= \mp\frac{2i\psi}{\omega}\left[\cos(\frac{1}{2}\omega t) + \frac{\omega^2 r^2}{8} e^{\pm i\omega t/2}\right] \\ R &= r\psi e^{\pm i\omega t/2}, \end{aligned} \tag{4.4}$$

gives the metric

$$\begin{aligned} ds^2 &= \psi^2\, dt^2 \;-\; \psi^2 e^{\pm i\omega t}(dr^2 \;+\; r^2 d\Omega^2) \;+\; \frac{4}{\omega^2} d\psi^2 \\ ds^2 &= \psi^2\, dt^2 \;-\; \psi^2 e^{\pm i\omega t}(dx^2 + dy^2 + dz^2) \;+\; \frac{4}{\omega^2} d\psi^2. \end{aligned} \tag{4.5}$$

Actually, this metric was first found without using the transformation (4.4), and each spatial component of the metric contained a spatial wave as well (e.g. $g_{xx} = -\psi^2 e^{\pm i(\omega t + k_x x)}$, etc.). However, it became apparent that the wavenumber

portion of the metric was insignificant when it came to examining the induced density and pressure (the components of T^{μ}_{ν} do not differ). Furthermore, it did not affect the fact that $R_{AB} = 0$ and $R_{ABCD} = 0$. Therefore, in this section we shall leave the metric in the isotropic form of (4.5). Where the difference comes into play is when geodesic motion is considered, and both metrics will be examined at that point.

That there are imaginary variables in the metric may seem to be disconcerting at first, although there have been previous studies using complex metrics [30, 31]. One can transform away any complex wavenumber portion (k_x, etc.), and one can also make the angular frequency imaginary to make the metric real, though this would change the physical interpretation of the metric (see below). However, even with a complex metric we find that the physical properties, such as density and pressure, are indeed real, as will now be shown.

For (4.5), the components of the induced energy-momentum tensor are

$$T^t_t = T^x_x = T^y_y = T^z_z = -\frac{3\omega^2}{4\psi^2}. \tag{4.6}$$

As in chapter 3, taking $\rho = T^t_t$ and $p = -\frac{1}{3}(T^x_x + T^y_y + T^z_z)$, the density and pressure of the fluid are

$$p = -\rho = \frac{3\omega^2}{4\psi^2}. \tag{4.7}$$

The equation of state is clearly that of a vacuum. We see that ordinary 3-space has a wave-like behavior, as well as the particles in the manifold (as will be shown in section 4.2), but the associated medium is an unperturbed vacuum. Hence, we feel it is appropriate to refer to this solution as vacuum waves.

In order for the metric to be flat, the signature of the ψ co-ordinate in (4.5) must be timelike, but it is also possible for it to be spacelike. If ω were to be imaginary, $-i\omega$, then the signature of $g_{\psi\psi}$ in (4.5) would reverse and the oscillation would become an exponential growth or decay, depending on the sign used. If the upper sign (+) in the exponential terms is used, then the metric, upon hypersurfaces $\psi = constant$, looks like a de Sitter inflationary model with a positive cosmological constant, $\Lambda = 3\omega^2/4\psi^2$. In its present form ($\omega$ real), the model is still a vacuum, only the spacetime is oscillating instead of inflating and the cosmological constant is negative.

Therefore, we could imagine the universe at a very early stage oscillating with a frequency $\omega/2\pi$. At a later time, ω becomes imaginary and (4.5) becomes inflationary. This is similar to other big-bang scenarios where the big bang is interpreted as a quantum-induced phase change [32, 33, 34]. In the inflationary mode, we note that the signature of $g_{\psi\psi}$ is the same as the other 5-D cosmological models described by (4.2).

Although is may seem odd that the physics depends on the co-ordinate frame chosen, there is a similar phenomenon in (3+1) cosmology. Here we have a covariant 5-D system which contains physical quantities defined in 4-D. In the (3+1) standard FRW models it is common to employ comoving co-ordinates where $\dot{x} = \dot{y} = \dot{z} = 0$. In this system, galaxies are static and there is no big bang. However, it is generally believed that galaxies are separating due to a universal expansion which is described in a non-comoving frame. The physical interpretation between the two frames is very different although both are perfectly valid in the 4-D theory. Here the theory is covariant in 5-D, but the 4-D cosmological models depend on the choice of co-ordinates used.

4.2 Geodesic Motion

In this section, for notation purposes, the upper sign (+) in the exponential of (4.5) will be used. The five geodesic equations for (4.5) are

$$\ddot{t} = -\frac{2}{\psi}\dot{t}\dot{\psi} - \frac{i}{2}\omega e^{i\omega t}\left[\dot{x}^2 + \dot{y}^2 + \dot{z}^2\right] \tag{4.8}$$

$$\ddot{x} = -\left(i\omega\dot{t} + \frac{2}{\psi}\dot{\psi}\right)\dot{x} \tag{4.9}$$

$$\ddot{y} = -\left(i\omega\dot{t} + \frac{2}{\psi}\dot{\psi}\right)\dot{y} \tag{4.10}$$

$$\ddot{z} = -\left(i\omega\dot{t} + \frac{2}{\psi}\dot{\psi}\right)\dot{z} \tag{4.11}$$

$$\ddot{\psi} = \frac{1}{4}\,\omega^2\psi\,\dot{t}^2 - \frac{1}{4}\omega^2\psi e^{i\omega t}\left[\dot{x}^2 + \dot{y}^2 + \dot{z}^2\right]. \tag{4.12}$$

The spatial velocities are easily integrated from (4.9)-(4.11) and are

$$\dot{x} = A_x \frac{e^{-i\omega t}}{\psi^2}, \quad etc. \tag{4.13}$$

Here, A_x is an integration constant. The velocities $\dot{y}$ and $\dot{z}$ have the same form as $\dot{x}$ but with different integration constants. Like the metric, particles in the manifold will be oscillating as well. However, when $\omega \to -i\omega$, then the metric is in an inflationary expansion but a particle's velocity components are exponentially decaying. Of course, in either case we could have a static 3-D spatial section by setting $A_x = A_y = A_z = 0$.

The energy, $\dot{t}$, was obtained by assuming $\dot{t} = V_0/\psi^2 + f_x(t,x)\dot{x} + f_y(t,y)\dot{y} + f_z(t,z)\dot{z}$ and then solving for f_x etc. Hence,

$$\dot{t} = \frac{1}{\psi^2}\left(V_0 - V_x x - V_y y - V_z z\right) \tag{4.14}$$

where $V_x = \frac{i\omega}{2}\tilde{A}_x\,A_x$, etc and $\tilde{A}_x$ is an integration constant established from the differential equations involving f_x, etc. If there is no motion in the spatial portion ($A_x = 0$, etc) then the system can be considered "comoving" on hypersurfaces of $\psi = constant$.

Finally, a particle's velocity in the extra dimension can be obtained from,

$$\Xi = \psi^2\,\dot{t}^2 \;-\; \psi^2 e^{i\omega t}(\dot{x}^2 + \dot{y}^2 + \dot{z}^2) \;+\; \frac{4}{\omega^2}\dot{\psi}^2,$$

where again Ξ is 1 for massive particles and 0 for massless particles. The velocity is hence

$$\dot{\psi} = \pm\frac{\omega}{2}\left[\Xi + \frac{A^2}{\psi^2}e^{-i\omega t} - \frac{1}{\psi^2}\left(V_0 - V_x x - V_y y - V_z z\right)^2\right]^{\frac{1}{2}}, \tag{4.15}$$

with $A^2 = A_x^2 + A_y^2 + A_z^2$.

As mentioned in the previous section, the metric (4.5) had been studied originally in the form

$$ds^2 = \psi^2\,dt^2 \;-\; \psi^2 e^{i\omega t}(e^{ik_X X}dX^2 + e^{ik_Y Y}dY^2 + e^{ik_Z Z}dZ^2) \;+\; \frac{4}{\omega^2}d\psi^2. \tag{4.16}$$

The difference between the two metrics manifests itself mostly in the geodesic motion. It is not necessary to recalculate the velocities from the new geodesic equations, but rather derive them from $\dot{X} \equiv dX/ds = \frac{\partial X}{\partial x}\frac{dx}{ds}$, etc. Noting that $x = \frac{2}{ik_X}e^{\frac{1}{2}ik_X X}$, etc, the new geodesic velocities are

$$\dot{t} \;=\; \frac{1}{\psi^2}\left(V_0 - V_X e^{\frac{1}{2}ik_X X} - V_Y e^{\frac{1}{2}ik_Y Y} - V_Z e^{\frac{1}{2}ik_Z Z}\right) \tag{4.17}$$

$$\dot{X} \;=\; \frac{A_x}{\psi^2}e^{-i\left(\omega t + \frac{1}{2}k_X X\right)} \tag{4.18}$$

$$\dot{Y} = \frac{A_y}{\psi^2} e^{-i\left(\omega t + \frac{1}{2} k_Y Y\right)} \tag{4.19}$$

$$\dot{Z} = \frac{A_z}{\psi^2} e^{-i\left(\omega t + \frac{1}{2} k_Z Z\right)} \tag{4.20}$$

$$\dot{\psi} = \pm \frac{\omega}{2} \Big[\Xi + A^2 e^{-i\omega t} \tag{4.21}$$

$$- \frac{1}{\psi^2} \left(V_0 - V_X e^{\frac{1}{2} i k_X X} - V_Y e^{\frac{1}{2} i k_Y Y} - V_Z e^{\frac{1}{2} i k_Z Z} \right)^2 \Big]^{\frac{1}{2}}, \tag{4.22}$$

where now $V_X = \frac{\omega}{k_X} A_x$, etc. Here we find that particles in the manifold also have spatial oscillations. Again, if we let $\omega \to -i\omega$ then during the inflationary phase, particles may oscillate in space anisotropically, but with a temporal damping due to the $e^{-\omega t}$ term. We hope to investigate whether oscillating charged particles in the de Sitter vacuum of the early universe could have generated the 3K microwave background.

Chapter 5

Conclusions

We began with examining the five-dimensional analogue of the Schwarzschild metric, modelling stellar sized objects, which is a class of solutions parameterized by two constants, ϵ and κ, which are restricted through $\epsilon^2(\kappa^2 - \kappa + 1) = 1$, $\kappa \geq 0$ and $\epsilon \geq 0$. The entire class, save one, lacks an event horizon, and we find that the centre can be defined to be at the conventional (3+1) event horizon. Further to strengthen this definition, we find that there exists a real scalar singularity at this point, physically restricting the manifold to outside this limit. The energy and velocities of a particle approaching this limit ($\tilde{r} = 2M$) diverge, whilst the velocity in the extra dimension slows to zero. The extra dimension itself has some fundamental length, ψ_o, at the origin and gets larger as one moves away from the spatial origin.

Previous work [17] has shown it possible to physically measure ϵ and κ and hence the effect of the extra dimension. In examining circular orbits, we find that not only do ϵ and κ play an important role in the physics, but also by a test particle's velocity in the extra dimension. This velocity is characterized by the integration constant V_0 of (2.17).

First we consider a substantial section of these class of objects, from the Schwarzschild limit ($\kappa \to \infty$) up to, but not including, the Chatterjee case ($\kappa = 1$). Here, massless particles with $V_0 = 0$ have one unstable circular orbit at radius $\tilde{r}_0 = [\epsilon(2\kappa - 1) + 1]M$, where $2M < \tilde{r}_0 \leq 3M$. Too large of a velocity in the fifth dimension makes it impossible for a particle, massless or massive, to have a circular orbit. The same is true if the angular momentum constant, L, is too small. At this extremum there is only one radius, $\tilde{r}_*$, in the manifold where a circular orbit can exist (the orbit is unstable). This radius lies in the range of $\tilde{r}_1 \leq \tilde{r}_* \leq \tilde{r}_2$, where $\tilde{r}_1 \equiv [3\epsilon(\kappa - 1) + 1 + \sqrt{4 - 3\epsilon^2\kappa}]M \in (2M, 6M]$ and $\tilde{r}_2 \equiv [\epsilon(3\kappa - 2) + 1 + \sqrt{3\epsilon^2\kappa^2 - 4\epsilon^2\kappa + 1}]M \in (2M, 6M]$, depending on the values of V_0, Ξ and L ($\tilde{r}_1 < \tilde{r}_2$ except in the Schwarzschild limit where $\tilde{r}_1 = \tilde{r}_2 = 6M$). Massless particles with $V_0 \neq 0$ have circular orbits similar to massive particles; both have stable orbits at radii $\tilde{r} > \tilde{r}_*$ and unstable orbits at radii $\tilde{r}_0 < \tilde{r} < \tilde{r}_*$.

The rest of the class of solutions (from Chatterjee, $\kappa = 1$, to "synchronous",

$\kappa = 0$) behave quite differently. First, there are no unstable orbits. Massless particles do not have circular orbits unless $V_0 \neq 0$, in which case the orbit is stable. Secondly, the circular orbits can exist at any radii in the manifold except, of course, at the origin, $\tilde{r} = 2M$. This offers a unique difference between the Schwarzschild case and the Chatterjee case where in both situations $\epsilon\kappa = 1$ and so some of their features are indistinguishable (e.g. particle energy, $\dot{t}$, and gravitational mass).

We next move onto larger scales and discover a metric that is a vacuum in five dimensions, but appears to give density and pressure profiles proportional to r^{-2} in four dimensions. The matter described is that of a inhomogeneous, static, isothermal cloud of matter, which is a good working model of many rich clusters of galaxies and superclusters. The system is parameterized by a constant α, which gives rise to various equations of state, $p = \frac{\alpha^2+2\alpha+2/3}{2-\alpha^2}\rho$, including dust with $\rho \neq 0$, which cannot be found in the four-dimensional analogue.

The "induced" gravitational mass is proportional to $\psi^{2+3/\alpha}$ and to $r^{2+\alpha}$. The density and mass physically restrict α to the range $[-1, 0) \cup (0, \sqrt{2}]$, but this restriction still allows for solutions of positive density and negative pressure, which does not occur in the four-dimensional case. We find that, except for $\alpha = -1$, a particle's energy drops to zero at spatial infinity.

Finally, on the largest scale, we discover a solution which has an oscillatory spatial portion with angular frequency ω. Upon examining the induced pressure and density, we find the metric describes an unperturbed de Sitter vacuum, and hence the solution can be called vacuum waves. If $\omega \to -i\omega$, then the metric looks like an inflating de Sitter model on hypersurfaces of $\psi = constant$. This metric is complimentary to that studied by Ponce de Leon and Wesson [28, 29], where the (4+1) metric can describe the universe at several epochs, but fails to incorporate an inflationary stage due to divergences in the metric.

For both metrics, it is possible to find a coordinate transformation that reduces the metric to a flat "Minkowski" one. This means that, in the right coordinates, cosmology is simpler in 5-D than in 4-D.

$\ddot{\smile}$

Appendix A

Christoffel Symbols and Riemann Tensor Components

For the solitons, the Christoffel symbols of the second kind for (2.1) are as follows:

$$\Gamma^t_{tr} = \frac{A'}{A} \qquad \Gamma^\psi_{\psi r} = \frac{C'}{C}$$

$$\Gamma^r_{tt} = \frac{AA'}{B^2} \qquad \Gamma^r_{rr} = \frac{B'}{B}$$

$$\Gamma^r_{\psi\psi} = -\frac{CC'}{B^2}$$

$$\Gamma^r_{\theta\theta} = -\frac{r^2BB' + rB^2}{B^2} \qquad \Gamma^r_{\phi\phi} = \Gamma^r_{\theta\theta}\ \sin^2\theta$$

$$\Gamma^\theta_{\theta r} = \Gamma^\phi_{\phi r} = \frac{r^2BB' + rB^2}{r^2B^2}$$

$$\Gamma^\theta_{\phi\phi} = -\sin\theta\cos\theta \qquad \Gamma^\phi_{\phi\theta} = \frac{\sin\theta}{\cos\theta}$$

where A, B and C are defined in (2.2)-(2.4) and $A' \equiv \partial A/\partial r$ etc. For this particular metric, there are 10 independent, non-zero Riemann tensor components:

$$
\begin{aligned}
R_{rtrt} &= (A''B - A'B')\frac{A}{B} \\
R_{t\theta t\theta} &= \frac{rAA'}{B}(rB' + B) = \frac{1}{\sin^2\theta}R_{t\phi t\phi} \\
R_{t\psi t\psi} &= \frac{AA'CC'}{B^2} \\
R_{r\theta r\theta} &= r^2(B')^2 - rBB' - r^2BB'' = \frac{1}{sin^2\theta}R_{r\phi r\phi} \\
R_{r\psi r\psi} &= -(C''B - B'C')\frac{C}{B} \\
R_{\theta\phi\theta\phi} &= -r^2\sin^2\theta B'(r^2B' + 2rB) \\
R_{\theta\psi\theta\psi} &= -\frac{rCC'}{B}(rB' + B) = \frac{1}{\sin^2\theta}R_{\phi\psi\phi\psi}
\end{aligned}
$$

For the isotrope solutions, the Christoffel symbols for (3.2) are:

$$
\begin{aligned}
\Gamma^t_{rt} &= (1+\alpha)/r & \Gamma^t_{\psi t} &= (1+3/\alpha)/\psi \\
\Gamma^r_{tt} &= \left(\frac{r}{r_o}\right)^{2(1+\alpha)}\psi^{2(1+3/\alpha)}\frac{(1+\alpha)}{(3-\alpha^2)\psi^2 r} & & \\
\Gamma^r_{r\psi} &= \frac{1}{\psi} & \Gamma^r_{\psi\psi} &= \frac{3r}{\alpha^2\psi^2} \\
\Gamma^r_{\theta\theta} &= -\frac{r}{3-\alpha^2} & \Gamma^r_{\phi\phi} &= \Gamma^r_{\theta\theta}\ \sin^2\theta \\
\Gamma^\theta_{r\theta} &= \Gamma^\phi_{r\phi} = \frac{1}{r} & \Gamma^\theta_{\psi\theta} &= \Gamma^\phi_{\psi\phi} = \frac{1}{\psi} \\
\Gamma^\theta_{\phi\phi} &= -\sin\theta\cos\theta & \Gamma^\phi_{\phi\theta} &= \frac{\sin\theta}{\cos\theta} \\
\Gamma^\psi_{tt} &= -\frac{\alpha^2}{3}\left(\frac{r}{r_o}\right)^{2(1+\alpha)}\psi^{2(1+3/\alpha)}\frac{(1+3/\alpha)}{(3-\alpha^2)\psi r^2} & &
\end{aligned}
$$

$$\Gamma^{\psi}_{r\psi} = \frac{1}{r} \qquad \Gamma^{\psi}_{rr} = \frac{\alpha^2\psi}{3r^2}$$

$$\Gamma^{\psi}_{\theta\theta} = \frac{\alpha^2\psi}{3(3-\alpha^2)} \qquad \Gamma^{\psi}_{\phi\phi} = \Gamma^{\psi}_{\theta\theta}\ \sin^2\theta$$

After the co-ordinate transformation (3.18) the Christoffel symbols for (3.19) are:

$$\Gamma^{t}_{tR} = \frac{R-\sqrt{3}\Psi}{R^2-\Psi^2} \qquad \Gamma^{t}_{t\Psi}\frac{\sqrt{3}R-\Psi}{R^2-\Psi^2}$$

$$\Gamma^{R}_{tt} = \frac{A}{3C}(R-\sqrt{3}\Psi)\left(\frac{R+\Psi}{R-\Psi}\right)^{\sqrt{3}} \qquad \Gamma^{R}_{\theta\theta} = -R/3$$

$$\Gamma^{R}_{\phi\phi} = \sin^2\theta\Gamma^{R}_{\theta\theta}$$

$$\Gamma^{\theta}_{R\theta} = \Gamma^{\phi}_{R\phi} = \frac{R}{R^2-\Psi^2} \qquad \Gamma^{\theta}_{\Psi\theta} = \Gamma^{\phi}_{\Psi\phi} = -\frac{\Psi}{R^2-\Psi^2}$$

$$\Gamma^{\theta}_{\phi\phi} = -\cos\theta\sin\theta \qquad \Gamma^{\phi}_{\theta\phi} = \frac{\cos\theta}{\sin\theta}$$

$$\Gamma^{\Psi}_{tt} = -\frac{A}{3C}(\sqrt{3}R-\Psi)\left(\frac{R+\Psi}{R-\Psi}\right)^{\sqrt{3}} \qquad \Gamma^{\Psi}_{\theta\theta} = -\Psi/3$$

$$\Gamma^{\Psi}_{\phi\phi} = \sin^2\theta\Gamma^{\Psi}_{\theta\theta}$$

For the vacuum solution, (4.5), the Christoffel symbols are

$$\Gamma^{t}_{xx} = \Gamma^{t}_{yy} = \Gamma^{t}_{zz} = \frac{i\omega}{2}e^{i\omega t} \qquad \Gamma^{t}_{t\psi} = 1/\psi$$

$$\Gamma^{x}_{tx} = \Gamma^{y}_{ty} = \Gamma^{z}_{tz} = \frac{i\omega}{2} \qquad \Gamma^{x}_{\psi x} = \Gamma^{y}_{\psi y} = \Gamma^{z}_{\psi z} = 1/\psi$$

$$\Gamma^{\psi}_{tt} = -\frac{\omega^2\psi}{4} \qquad \Gamma^{\psi}_{xx} = \Gamma^{\psi}_{yy} = \Gamma^{\psi}_{zz} = \frac{\omega^2\psi}{4}e^{i\omega t}.$$

The Christoffel symbols for the anisotropic version of the vacuum waves,

(4.16), are

$$\Gamma^t_{XX} = \frac{i\omega}{2} e^{i(\omega t + k_X X)} \ (etc.) \qquad \Gamma^t_{t\psi} = 1/\psi$$

$$\Gamma^X_{tX} = \Gamma^Y_{tY} = \Gamma^Z_{tZ} = \frac{i\omega}{2} \qquad \Gamma^X_{\psi X} = \Gamma^Y_{\psi Y} = \Gamma^Z_{\psi Z} = 1/\psi$$

$$\Gamma^X_{XX} = \frac{ik_X}{2} \ (etc.)$$

$$\Gamma^\psi_{tt} = -\frac{\omega^2 \psi}{4} \qquad \Gamma^\psi_{XX} = \frac{\omega^2 \psi}{4} e^{i(\omega t + k_X X)} \ (etc.).$$

Appendix B

Subroutines Written for MapleV

The following set of subroutines are written in conjuction with Maple V software. Particularly, it is to be used with the tensor library (or GRTensor library supplied by Kayll Lake at Queen's University). In Maple V, this file is read using the command "read mapadd;". After having done this, the file first calls up Maple V's library "tensor" in case the library hasn't already been called. Afterwhich it will list all the available subroutines that are in the file. Any procedure desired to be used is then called up by typing its name followed by an empty set of parentheses. For example, to use the subroutine addoneD, one would type "addoneD();". The file mapadd can be found on a 3.5″ floppy at the end of the thesis.

```
#######################################################################
```

```
#
# File mapadd is used in MapleV by using the command read mapadd;
# The file first calls MapleV's library tensor and then defines new
# subroutines to be used with tensor.
#
#####################################################################
readlib(tensor):
#
# addoneD() adds one extra dimension to the metric, Ndim=Ndim+1, and
# makes sure all the new off diagonal terms is zero
#
addoneD := proc () local i; global x1,x2,x3,x4,x5,g11,g22,g33,
g44,Ndim; option `Copyright 1994 by APB`;
if Ndim=4 then Minkowski(); fi;
Ndim:=Ndim+1;x5:=Y:
for i from 1 to Ndim-1 do: g.i.Ndim:=0:g.Ndim.i:=0: od;
NULL end;
#
# cartesian() makes sure the first coordinate is time (in the tensor
# library time is the 4th coordinate) and then makes the subsequent
# three coordinates x, y and z (the 3-space metric components are
# flat)
#
cartesian:=proc() global x1,x2,x3,x4,g22,g33,g44; option `Copyright
                                                        1994 by APB`;
x1:=t:x2:=x:x3:=y:x4:=z:
g22:=-1:g33:=-1:g44:=-1:
NULL end;
#
# display2() acts the same way as display in tensor, except the
# indices are written as the coordinates and not numbers. i.e. gtt
# instead of g11.
#
display2 := proc (a) local i, j, k, l, t, z, s; option `Copyright 1994
by APB`;
if nargs = 0 then
display2(dimension); display2(coordinates); display2(metric);
display2(detmetric); display2(invmetric); display2(Christoffel1);
display2(Christoffel2); display2(Riemann); display2(Ricci);
```

```
display2(Ricciscalar);display2(Kretchmann); display2(Einstein);
display2(Weyl); RETURN()
fi; z := true;
if a = metric then print(`covariant metric tensor components`);
for i to Ndim do for j from i to Ndim do
if g.i.j <> 0 then print(` g `.(x.i).` `.(x.j) =g.i.j); z := false fi
od od
elif a = invmetric then print(`contravariant metric tensor
components`);
for i to Ndim do for j from i to Ndim do
if h.i.j <> 0 then print(` h `.(x.i).` `.(x.j) = h.i.j); z := false fi
od od
elif a = induced then print(`covariant components of induced energy
momemtum tensor`);
for i to 4 do for j from i to 4 do
if T.i.j <> 0 then print(` T `.(x.i).` `.(x.j) = T.i.j); z := false fi
od od
elif a = Ricci then print(`covariant Ricci tensor components`);
for i to Ndim do for j from i to Ndim do
if R.i.j <> 0 then print(` R `.(x.i).` `.(x.j) = R.i.j); z := false fi
od od
elif a = Einstein then print(`covariant Einstein tensor components`);
for i to Ndim do for j from i to Ndim do
if G.i.j <> 0 then print(` G `.(x.i).` `.(x.j) = G.i.j); z := false fi
od od
elif a = Christoffel1 then print(`Christoffel symbols of the first
kind`);
for i to Ndim do for j from i to Ndim do for k to Ndim do
if c.i.j.k <> 0 then print(` c `.(x.i).` `.(x.j).` `.(x.k) = c.i.j.k);
z := false fi od od od
elif a = Christoffel2 then print(`Christoffel symbols of the second
kind`);
for k to Ndim do for i to Ndim do for j from i to Ndim do
if C.i.j.k <> 0 then print(` C `.(x.i).` `.(x.j)^(x.k) = C.i.j.k); z
 := false fi od od od
elif a = Riemann then print(`covariant Riemann tensor components`);
for i to Ndim-1 do for j from i+1 to Ndim do for k from i to Ndim-1 do
if k = i then t := j else t := k+1 fi;
for l from t to Ndim do
```

```
if R.i.j.k.l <> 0 then print(` R `.(x.i).` `.(x.j).` `.(x.k).` `.(x.l)
= R.i.j.k.l); z := false fi od od od od
elif a = Weyl then print(`covariant Weyl tensor components`);
for i to Ndim-1 do for j from i+1 to Ndim do for k from i to Ndim-1 do
if k = i then t := j else t := k+1 fi; for l from t to Ndim do
if C.i.j.k.l <> 0 then print(` C `.(x.i).` `.(x.j).` `.(x.k).` `.(x.l)
= C.i.j.k.l); z := false fi od od od od
elif a = Ricciscalar then print(`Ricci scalar`);  print (` R` = R);
z := false
elif a = Kretchmann then print(`Kretchmann scalar`); print (` K` = K);
z := false
elif a = dimension then print(`dimension of the space`); print(` Ndim`
= Ndim); z := false
elif a = coordinates then print(`the coordinates are`);
print(seq(` x `.i = x.i,i = 1 .. Ndim)); z := false
elif a = detmetric then print(`determinant of the covariant metric
tensor`); print(` detg` = detg); z := false
else ERROR(`argument must be one of:`,'dimension','coordinates',
'metric','detmetric','invmetric','Christoffel1','Christoffel2',
'Riemann','Riemann2','Ricci','Ricciscalar','Kretchmann','induced',
'Einstein','Weyl','NULL') fi; if z then print(a = `All components are
zero`) fi; NULL end;
#
# identity() performes the operation gij*hjk (covariant metric
# contracted with contravariant metric).  If the contravariant metric
# is correct then a Ndim dimensional Kronecker delta is obtained.
# This is used when the contravariant metric is inputted by hand and
# not calculated using invmetric() in tensor; identity() then checks
# to see if hij is indeed the contravariant form of gij
#
identity:=proc() local i,j; global Ndim; option `Copyright 1994
                                                                by APB`;
for i from 1 to Ndim do;
for j from 1 to Ndim do;
Q.i.j:=factor(simplify(sum('h.i.k*g.j.k','k'=1..Ndim)));
od od;
print (`Identity matrix if all goes well:`);
for i from 1 to Ndim do;
print (seq(Q.i.j,j=1..Ndim));
```

```
od;
NULL end;
#
# induced() calculates the four dimensional induced matter energy-
# momemtum tensor.  The equation is obtained from section IV of
# ``Exact Solutions and# the Effective Equation of State in Kaluza-
# Klein Theory'' by J. Ponce de Leon and P.S. Wesson (J. Math. Phys.
#  _34_, 4080 (1993)).
#
induced := proc () local i, j,a1,a2,a3,a4,a5,a6,a7, s; option
`Copyright 1994 by APB`;
s:=g55:
for i from 1 to 4 do;
for j from i to 4 do;
  T.i.j:=0;T.j.i:=0;
od od;
print (`calculating induced energy momentum tensor`);
for i from 1 to 4 do;
for j from 1 to 4 do;
  printf(`%-s\n`,` T`.i.j.` `);
  a1:=diff(s,x.i,x.j)/(2*s)-diff(s,x.i)*diff(s,x.j)/(4*s^2)
                        -sum('C.i.j.k*diff(s,x.k)/(2*s)','k'=1..4);
  a2:=1/(2*s)*diff(s,x5)*diff(g.i.j,x5)/(2*s);
  a3:=1/(2*s)*diff(g.i.j,x5$2);
  a4:=1/(2*s)*(sum('sum('h.k.l*diff(g.i.k,x5)*diff(g.j.l,x5)',
                                            'k'=1..4)','l'=1..4) );
  a5:=1/(2*s)*(sum('sum('h.k.l/2*diff(g.k.l,x5)*diff(g.i.j,x5)',
                                            'k'=1..4)','l'=1..4) );
  a6:=1/(2*s)*g.i.j/4*(sum('sum('diff(h.k.l,x5)*diff(g.k.l,x5)',
                                            'k'=1..4)','l'=1..4) );
  a7:=1/(2*s)*g.i.j/4*(sum('sum('h.k.l*diff(g.k.l,x5)','k'=1..4)',
                                                      'l'=1..4) )^2;
  T.i.j:=simplify(a1-a2+a3-a4+a5-a6-a7);
od od;
  printf(`%-s\n`,` `);
NULL end;
#
# Minkowski returns the 4-D part of the metric to a Minkowski metric,
# with time as the first coordinate and a signature of (+---).
```

```
# Cartesian coordinates are used.
#
Minkowski:=proc() local i,j; global Ndim,al,x1,x2,x3,x4,g11,g12,g13,
 g14,g21,g22,g23,g24,g31,g32,g33,g34,g41,g42,g43,g44; option
`Copyright 1994 by APB`;
Ndim:=4:for i from 1 to Ndim do:for j from 1 to Ndim do:
g.i.j:=0: od od:
g11:=1:g22:=-1:g33:=-1:g44:=-1:x1:=t:x2:=x:x3:=y:x4:=z:
NULL end;
#
# PonceDeLeon() creates the metric which describes the five
# dimensional cosmological solutions developed in Ponce de Leon,
# Gen. Rel. Grav. _20_, 539 (1988).
#
PonceDeLeon:=proc() global Ndim,al,x1,x2,x3,x4,x5,g11,g22,g33,g44,g55;
option `Copyright 1994 by APB`;
Minkowski(): addoneD():cartesian():
g11:=Y^2:g55:=-al^2/(1-al)^2*t^2:
g22:=-t^(2/al)*Y^(2/(1-al)):g33:=-t^(2/al)*Y^(2/(1-al)):
g44:=-t^(2/al)*Y^(2/(1-al)):
display2(metric):
NULL end;
#
# Riemann2() calcuates the Riemann tensor with the first index raised.
#
Riemann2 := proc () local i, j, k, l, t,s ; option `Copyright 1994 by
APB`;
print (` calculating Rieman tensor in the form R`^` a`*`b c d`);
for i to Ndim-1 do
for j from i+1 to Ndim
do for k from i to Ndim-1 do if k = i then t := j else t := k+1 fi;
for l from t to Ndim do
if R.i.j.k.l <> 0 then
  s:=normal(sum('R.q.j.k.l*h.i.q','q'=1..Ndim)):
  RR.i.j.k.l:=s: RR.k.l.i.j:= s: RR.j.i.l.k := s: RR.l.k.j.i := s:
  RR.j.i.k.l := -s: RR.i.j.l.k := -s: RR.k.l.j.i := -s:
  RR.l.k.i.j := -s:
fi od od od od;
NULL end;
```

```
#
# Similar_5d() creates the five dimensional metric that describes a
# 4-D fluid with pressure and density proportional to r^(-2).  This
# metric is used to describe such systems as clusters and
# superclusters of galaxies.
#
Similar_5d:=proc() global Ndim,al,x1,x2,x3,x4,x5,g11,g22,g33,g44,g55;
option `Copyright 1994 by APB`;
Minkowski(): addoneD():spherical():
g11:=(r/ro)^(2*(a+1))*Y^(2*(a+3)/a):g55:=3*(3-a^2)/a^2*r^2:
g22:=-(3-a^2)*Y^2:g33:=-Y^2*r^2:g44:=-Y^2*r^2*sin(th)^2:
display2(metric):
NULL end;
#
# spherical() makes sure the first coordinate is time (in the tensor
# library time is the 4th coordinate) and then makes the subsequent
# three coordinates r, th (for theta) and ph (for phi) (the 3-space
# metric components are spherical coordinates but flat)
#
spherical:=proc() global x1,x2,x3,x4,g22,g33,g44; option `Copyright
                                                          1994 by APB`;
x1:=t:x2:=r:x3:=th:x4:=ph:
g22:=-1:g33:=-r^2:g44:=-r^2*sin(x3)^2:
NULL end;
#
# Vacuum_5d() creates the five dimensional metric that describes a
# 4-D de Sitter vacuum (p=-rho) with oscillating 3-D spatial section.
#
Vacuum_5d:=proc() global Ndim,al,x1,x2,x3,x4,x5,g11,g22,g33,g44,g55;
option `Copyright 1994 by APB`;
Minkowski(): addoneD():cartesian():
g11:=Y^2:g55:=4/w^2:
g22:=-Y^2*exp(I*w*t):g33:=g22:g44:=g22:
display2(metric):
NULL end;
```

References

[1] T. Kaluza, Sitzungsber. Press. Akad. Wiss. **33**, 966 (1921).

[2] O. Klein, Z. Phys. **37**, 895 (1926).

[3] P.S. Wesson, Astrophys. J. **394**, 19 (1992).

[4] P.S. Wesson and J. Ponce de Leon, J. Math. Phys. **33**, 3883 (1992).

[5] D. McManus, J. Math. Phys. **35**, 4889 (1994).

[6] B. Mashhoon, H. Liu, and P.S. Wesson, Phys. Lett. B **331**, 305 (1994).

[7] J.M. Overduin and P.S. Wesson, Phys. Rep., in preparation (1995).

[8] P.S. Wesson, H. Liu, Astrophys. J. **440**, 1 (1995).

[9] J. Ponce de Leon and P.S. Wesson, J. Math. Phys. **34**, 4080 (1993).

[10] D.J. Gross and M. J. Perry, Nucl. Phys. B **226**, 29 (1983).

[11] A. Davidson and D. Owen, Phys. Lett. B **155**, 247 (1985).

[12] T. Dereli, Phys. Lett. B**161**, 307 (1985).

[13] S. Chatterjee, Astron. Astrophys. **230**, 1 (1990).

[14] H.Y. Liu, Gen. Relativ. Gravit. **23**, 759 (1991).

[15] L.D. Faddeev and L.A. Takhtajan, in *Hamiltonian Methods in the Theory of Solitons* (Springer, Berlin, 1987).

[16] P.S. Wesson, "Kaluza-Klein Gravity and Step", Report, Physics, Stanford Un. (1993).

[17] D. Kalligas, P.S. Wesson and C.W.F. Everitt, Ap. J. **439**, 548 (1994).

[18] L. Sokolowski and B.J. Carr, Phys. Lett. B **176**, 334 (1986).

[19] P.S. Wesson, Phys. Lett. B **276**, 299 (1992).

[20] P.S. Wesson and J. Ponce de Leon, Class. Quant. Grav. **11**, 1341 (1994).

[21] P.S. Wesson and P. Lim, Astron. Astrophys **261**, 373 (1992).

[22] A.P. Billyard, D. Kalligas and P.S. Wesson, Int. J. Mod. Phys. (in press).

[23] R.N. Henriksen and P.S. Wesson, Astrophys. Space Sci. **53**, 429 (1977).

[24] R.N. Henriksen and P.S. Wesson, Astrophys. Space Sci. **53**, 445 (1977).

[25] W.B. Bonnor, Gen. Rel. Grav. **21**, 1143 (1989).

[26] W.B. Bonnor and F.I. Cooperstock, Phys. Lett. A **139**, 442 (1989).

[27] J.M. Overduin, P. Lim and P.S. Wesson, *in* Proc. 7th Marcel Grossman Meeting on General Relativity (ed. Kaiser, M.), World Scientific, Singapore, in press (1995).

[28] P.S. Wesson and J. Ponce de Leon, Gen. Rel. Grav. **26**, 555 (1994).

[29] P.S. Wesson, Astrophys. J. **394**, 19 (1992).

[30] J. Plebanski, J. Math. Phys. **16**, 2395 (1975).

[31] J. Plebanski, J. Math. Phys. **18**, 2511 (1977).

[32] A. Vilenkin, Phys. Rev. D **117**, 25 (1982).

[33] P.S. Wesson, Astron. Astrophys. **151**, 276 (1985).

[34] A. Linde, Physica Scripta T **36**, 30 (1991).